

Greenlandic Ice Cap Water

Technical Report on five potential locations for meltwater export

Andreas P. Ahlstrøm, Christian N. Albers, Signe B. Andersen,
Camilla s. Andresen, Dirk van As, Michele Citterio,
Robert S. Fausto, Karina Hansen, Bent Hasholt,
Anders R. Johnsen, Kristian K. Kjeldsen
& Anne M. Solgaard



Greenlandic Ice Cap Water

Technical Report on five potential locations for meltwater export

Andreas P. Ahlstrøm, Christian N. Albers, Signe B. Andersen,
Camilla S. Andresen, Dirk van As, Michele Citterio,
Robert S. Fausto, Karina Hansen, Bent Hasholt,
Anders R. Johnsen, Kristian K. Kjeldsen
& Anne M. Solgaard

Contents

1.	Summary	4
2.	Introduction	5
3.	Selection of potential locations	6
4.	Accessibility assessment	9
4.1	Sea ice and iceberg conditions	9
4.2	Bathymetry	11
5.	Glaciological analysis	20
5.1	Catchment delineation and change risk assessment	20
5.2	Risk assessment of glacial lake outburst floods	21
5.3	Runoff from meltwater and precipitation	22
5.4	Estimation of the age of the meltwater source ice	27
5.4.1	Ice-dynamic model setup	28
5.4.2	Estimated age of the ice	30
6.	Results from the water quality analysis	34
6.1	Sampling methodology	34
6.2	Inorganic parameters including selected trace metals	38
6.3	Radioisotopes	40
6.4	Bacterial counts	41
6.5	Cyanotoxins	44
6.6	Sediment content	45
7.	Conclusion	48
8.	References	49

1. Summary

Meltwater from Greenland is an increasingly attractive resource of pure freshwater. To attract investments from the industry, an extensive effort has been launched to map possible extraction locations, determine the quality of the meltwater, and review the existing ice and water export legislation. This report presents results from mapping- and water quality analysis of five selected locations, visited by boat in June 2017. Two locations drain ice sheet catchments and three locations drain catchments with local mountain glaciers.

The mapping includes catchment delineation, ice- and land runoff modelling, ice-dynamic modelling of the age of the melting ice, collection of fjord depth data and an assessment of the risk from glacial lake outburst floods. An extensive analysis of chemical, physical and microbiological parameters were performed on the water samples collected during field-work. Some types of analysis had to be performed on-site, some were performed at GEUS laboratories, and some at certified commercial laboratories.

Greenland has a diverse geology including areas with potential for mining of metals and radioactive isotopes. The existence of such areas could influence the water quality in meltwater rivers. The 2017 survey, however, showed excellent water quality at all locations with regards to inorganics like metal ions and radioisotopes. Toxic metals like arsenic, cadmium and nickel were well below the lowest criterion at all locations and so was fluoride, which may be an indicator for a number of toxic metals in Southern Greenland. Radioactivity was below the detection limit of the commercial laboratory at all locations. The seasonal variation of metals and radioisotopes is not yet known, but so far the locations look promising with regards to these quality parameters.

Biology is another factor that may influence water quality of meltwater rivers. Of most concern are cyanobacteria in lakes and rivers and bacteria from the gut of animals. Cyanobacteria produce toxins like microcystins and Anatoxin-A. These compounds were not detected at any of the locations. Coliforms and enterococci were chosen as indicator bacteria. Coliforms were not found at any location. *Enterococcaceae* were detected only at one location (2 per 5 mL). Total colony forming units (CFU) at 22 and 36°C were also analysed. While some CFU were found at 22°C (7-115 per mL) almost none were found at 36°C (0-2 per mL), which is a good safety indication. The bacterial parameters generally indicated good water quality, but some sort of simple disinfection should be considered, as is the case for all surface water for human consumption.

In summary, the results indicate an excellent water quality at all five locations, with all parameter values below the required drinking water standards for the European Union, the United States and The International Council of Bottled Water Associations (ICBWA).

2. Introduction

Drinking water of high quality is becoming a scarce resource worldwide. As the world population grows, demand is rising while the supply is under pressure from the impact of climate change. In Greenland, pure meltwater running off the Greenland Ice Sheet provides the solution. As the annual hydrological cycle intensifies with higher temperatures in the Arctic, the available water resource only increases. Unlike mountain glaciers which are vanishing globally, the Greenland Ice Sheet is vast, containing 2,85 million cubic kilometres of pure glacier ice providing a freshwater reservoir without equal in the northern hemisphere.

The Greenland Ice Sheet covers most of the land in Greenland with rivers transporting the meltwater a short distance through the mountains to the fjords through the largely uninhabited country. Due to limited sea ice, the fjords in Southwestern Greenland provide direct access by ship to the meltwater river mouths.

The Government of Greenland actively supports the prospect of drinking water export from this immense resource. To attract investments from the industry, an extensive effort has been launched to map possible extraction locations, determine the quality of the meltwater and review the existing ice and water export legislation.

Mapping and water quality assessments are undertaken by the Geological Survey of Denmark and Greenland (GEUS) adhering to the highest international standards. GEUS has been charged by the Government of Greenland to identify suitable locations for extraction of drinking water from meltwater rivers, conduct field investigations and water sampling, and subsequently carry out water quality assessments in certified laboratories. GEUS is the National Data Centre for water quality information for all of Denmark's more than 280,000 drinking water wells and has carried out extensive geoscientific fieldwork in Greenland since 1946.

3. Selection of potential locations

Locations are defined as outlets of significant meltwater rivers to accessible fjords in the southwestern part of Greenland, to minimize potential sea ice and iceberg interference. The initial assessment of locations was based on a three-level approach, evaluating in turn accessibility, abundance, and water quality, respectively. For each of these three levels, five different criteria were identified and assigned a weight in the assessment with the goal to single out the most promising locations to visit in the field.

The accessibility criteria includes proximity to infrastructure, marine chart coverage, availability of bathymetry data, and abundance of sea ice and icebergs, respectively. The abundance criteria relates to water discharge, length of the melt season, existence of proglacial lakes, risk of outburst floods, and upstream catchment changes. Finally, the water quality criteria focuses on origin of the water, age of the source ice, expected sediment concentration in the meltwater, and other issues from contact with naturally occurring minerals.

Each location was meticulously examined and rated with respect to the 15 criteria from the considerable geospatial, geological and geochemical datasets available to the Government of Greenland and GEUS. The criteria, sorted by level, and their graduation and weight are illustrated in Table 1. The rating of a location assigns a number, moderated by the a relative weight, for each criterion. The outcome is a ranking of the locations, which in turn is used to select the most promising locations to visit in the field for water sampling and further data collection.

Criterion	Poor 5	Mainly poor 4	Useful 3	Mainly good 2	Good 1	Weight	
Accessibility	Proximity to infrastructure	Unknown/sporadic access from marine/land side and/or >100 km	Occasional access from the marine side in the operational part of the season, and/or >100 km	Access possible from marine side in the operational part of the season	<25 km with access possible from the marine side all year round	Access by road all year round	Low
	Marine chart coverage	No charts	In proximity of older charts	In proximity of recent charts	Older charts	Recent charts	Low
	Bathymetry	Known shallow waters	No nearby data - estimated risk of shallow waters	No nearby data - estimated deep waters to the coast	Assumed deep water to coast based on experience and nearby data	Deep waters directly to the coast known	High
	Sea ice	Occasional blocking sea ice and fjord ice	Occasional blocking fjord ice	Occasional blocking sea ice	Narrow fjord access, ice-free ocean	Open fjord, ice-free ocean	High
	Icebergs	In fjord with calving glacier and some icebergs in ocean	In fjord with minor calving glacier and some icebergs in ocean	In fjord with minor calving glacier and few icebergs in ocean	No calving glacier in fjord and some icebergs in ocean	No calving glacier in fjord and few icebergs in ocean	High
Abundance	Discharge	Small catchment with no ice cover	Small catchment with partial ice cover	Large catchment with minor ice cover	Large catchment with partial ice cover	Very large catchment with partial inland ice sheet cover	Medium
	Length of melt season	Northwestern	Western	Southwestern	Southern, with small lake	Southern, with large lake	Medium
	Proglacial lake	No lake	Small lake	Several small lakes	Large lake	Several large lakes	Medium
	Outburst floods	Clear indications of outburst flood from lake	Likely outburst flood from lake	Lake with adjoining ice cover, but outburst flood less likely	Outburst flood not likely, but small lake with adjoining ice cover	No lakes with adjoining ice cover	High
	Catchment change	Small catchment with significant risk of change	Small catchment with some risk of change	Large catchment with risk of change	Large catchment with low risk of change over ice cover	Very large catchment on the inland ice (change not important)	Medium
Water quality	Origin of water	Primarily from ice-free catchment	Primarily from local ice cover (not inland ice)	Both from local glaciers and inland ice	Primarily meltwater from the inland ice	Almost exclusively meltwater from the inland ice	Low
	Age of ice source	Minor local glacier	Primarily from local ice cap	Both from local glaciers and inland ice	Younger inland ice	Older inland ice	Low
	Sediment concentration	Extremely high (>2000 mg/L)	High (1000-2000 mg/L)	Medium (300-1000 mg/L)	Low (50-300 mg/L)	Weak (<50 mg/L)	Low
	Radioactivity	High concentration	Medium-high concentration	Medium concentration	Medium-low concentration	Low concentration	High
	Inorganic compounds	High concentration	Medium-high concentration	Medium concentration	Medium-low concentration	Low concentration	High

Table 1. The 15 criteria sorted by the three levels (accessibility, abundance and water quality) and the specific graduation into five levels. The column to the right assigns a weight to each criterion with respect to the others.

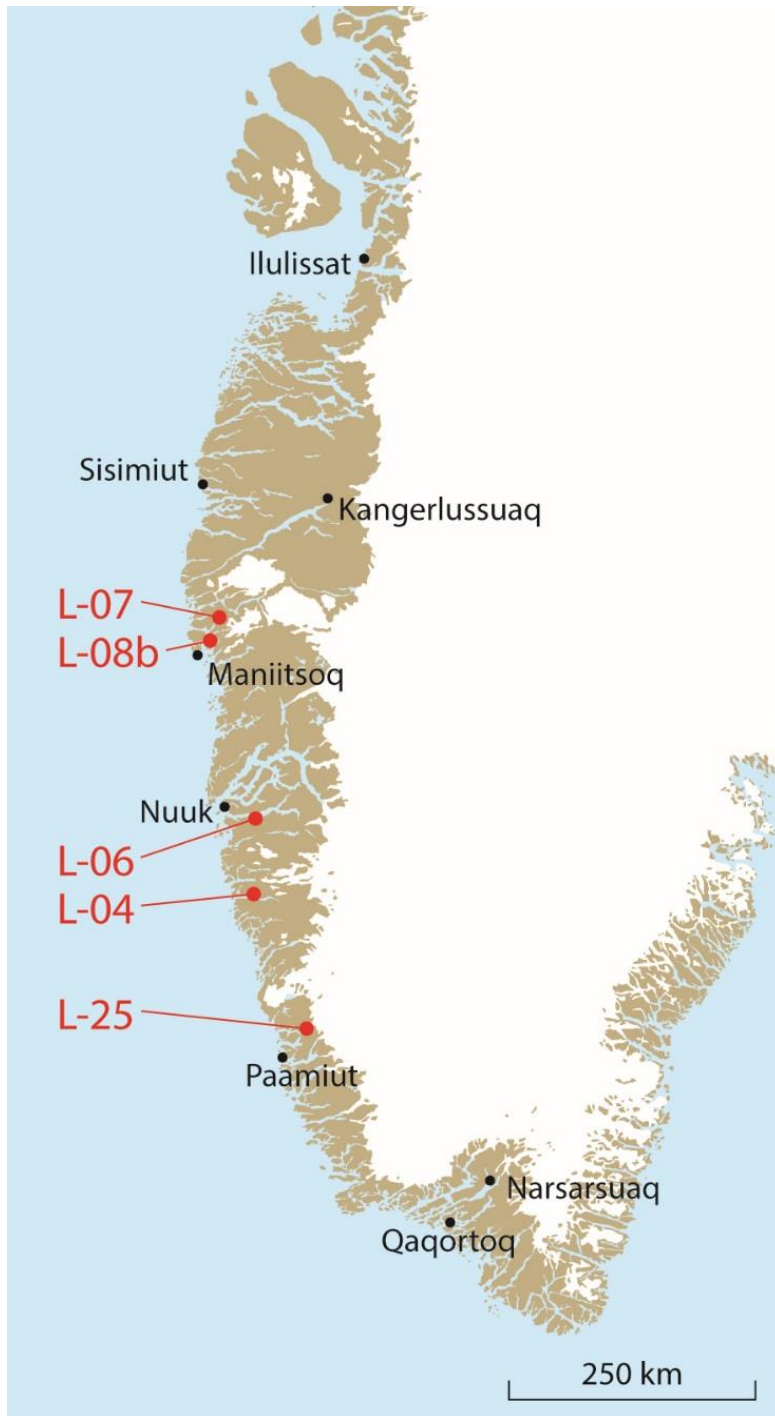


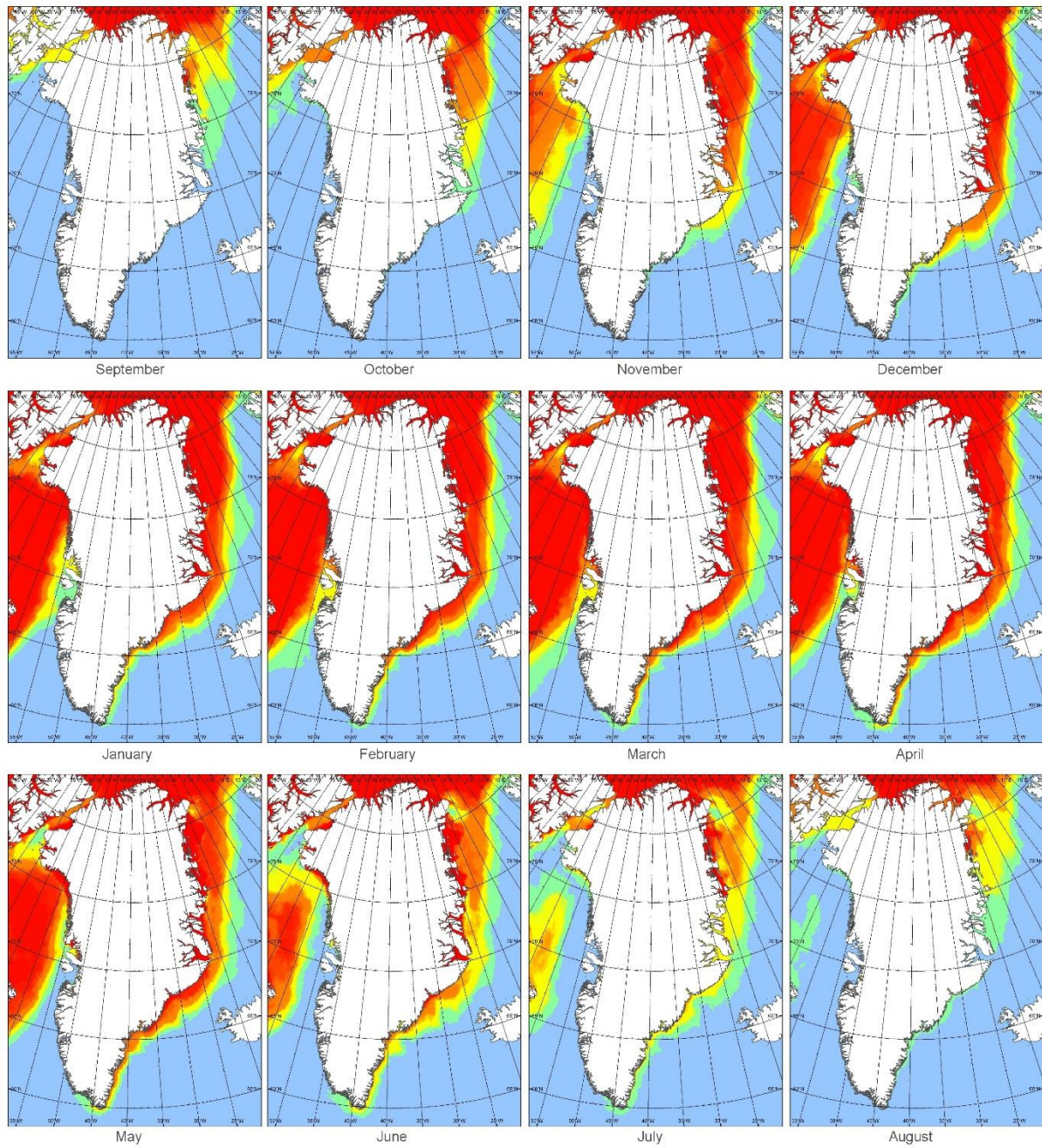
Figure 1. Overview map of the 5 locations selected through the ranking process.

4. Accessibility assessment

An intimate knowledge of the sailing conditions is crucial in order to determine whether a location is suitable for meltwater collection. Primary parameters to be assessed includes bathymetry, nearby ports, fjord ice conditions, sea ice and iceberg occurrence, which together determine what kind of ship or vessel is appropriate for a given location. Currently, five ports in South and Southwest Greenland, i.e. in the vicinity of the selected locations, service shipping over the Atlantic Ocean: Sisimiut, Nuuk, Narsaq, Qaqortoq and Nanortalik. These ports have a maximum capacity between 550 and 3300 TEU. The most proximate port to most locations is Nuuk, which is also the largest of the ports.

4.1 Sea ice and iceberg conditions

Conditions for sea ice and icebergs vary over the extensive southwestern Greenland coastline. In South Greenland, the ice present mainly consists of sea ice and glacier ice transported down along the East Greenland coast with the East Greenland current where it eventually flows around Kap Farvel (Cape Farewell). South Greenland is generally free from sea ice from August to December, while icebergs can be expected year-round. Unlike the sea ice in South Greenland, the sea ice in Southwest Greenland is produced locally during the winter. Icebergs are present year-round, but more so to the north near Disko Bay, where calving glaciers are more proliferate. According to the Danish Meteorological Institute (DMI), it is normally possible to sail to Aasiaat and Ilulissat from around May to December. The monthly mean concentration of sea ice around Greenland for the time period 2000-2010 is shown in Fig. 2, which illustrates the difference between South and Southwest Greenland and also that a significant part of the coast towards Disko Bay remains relatively ice free for significant parts of the year. Still, icebergs are present year-round. All the locations selected are situated in the part of Greenland least affected by sea ice and icebergs, and thus optimal for transportation and the length of extraction season, evaluated on the basis of the maps shown in Fig. 2 and maps from DMI's ice mapping service in the Kap Farvel region and southwestern Greenland for the period April 2010 to February 2017.



Colour code	Total concentration WMO Nomenclature
Blue	< 1/10 (open water)
Light Green	1/10 - 3/10 (very open ice)
Yellow	4/10 - 6/10 (open ice)
Orange	7/10 - 8/10 (close ice)
Red	9/10 - 10/10 (very close ice)

© 2007 METEO SERVICE - DMI - FRODO - MARINE SERVICE - 21/06/10 13:31:02

Figure 2. Monthly mean sea ice concentration derived from Greenland overview ice charts over the time period 2000-2010.

4.2 Bathymetry

The international bathymetric surveying carried out around Greenland (IBCAO, International Bathymetric Chart of the Arctic Ocean) does not cover the Greenlandic fjords adequately. Generally, routing of larger vessels take place only through regions with bathymetric charts suitable for navigation. By special agreement with the Danish Geodata Agency we have been granted access to yet unpublished bathymetric charts for the regions where these are so far available. A more thorough survey of the fjords in Greenland is currently underway, but not yet completed. To ensure the best possible evaluation of the access to the selected locations, we also included unpublished water depth observations collected from a range of sources by the Greenland Institute of Natural Resources (K. Brix Zinglensen). These water depth data cover a wider region than the bathymetric charts of the Danish Geodata Agency and are often the only data source in the vicinity of the selected locations. However, these data are not tied to a vertical reference surface (e.g. MSL, LAT, geoid, ellipsoid), implying that no corrections, e.g. tidal corrections, etc., have been applied, but generally just indicates the water depth below a ship at a given time. Thus, data should be used with caution and only as an indication of accessibility of a given location and not for navigational purposes.

Summarizing, the observations of water depth presented Figs. 3–10 are derived from three datasets:

1. A dataset from the Greenland Institute of Natural Resources, which consists of single beam water depth data from tour boats and trawlers recorded during navigation, not originally intended as bathymetric measurements. These are generally depicted as lines, or rather a series of point measurements. Kindly provided by Karl Brix Zinglensen (GNRI).
2. A bathymetric dataset from the Danish Geodata Agency recorded with multibeam sonar. These data provide full areal coverage when available. Kindly provided by Danish Geodata Agency.
3. A dataset resembling (1) above, recorded from the boat during fieldwork.

Note that datasets (1) and (3) are not proper bathymetric datasets and have not been corrected for tidal water level differences. They are only intended to provide an indication of the likely accessibility by ship and may not be relied on for actual navigational purposes. The water depth presented in Figs. 3-10 illustrate the minimum water depth within 100 m x 100 m grid cells.

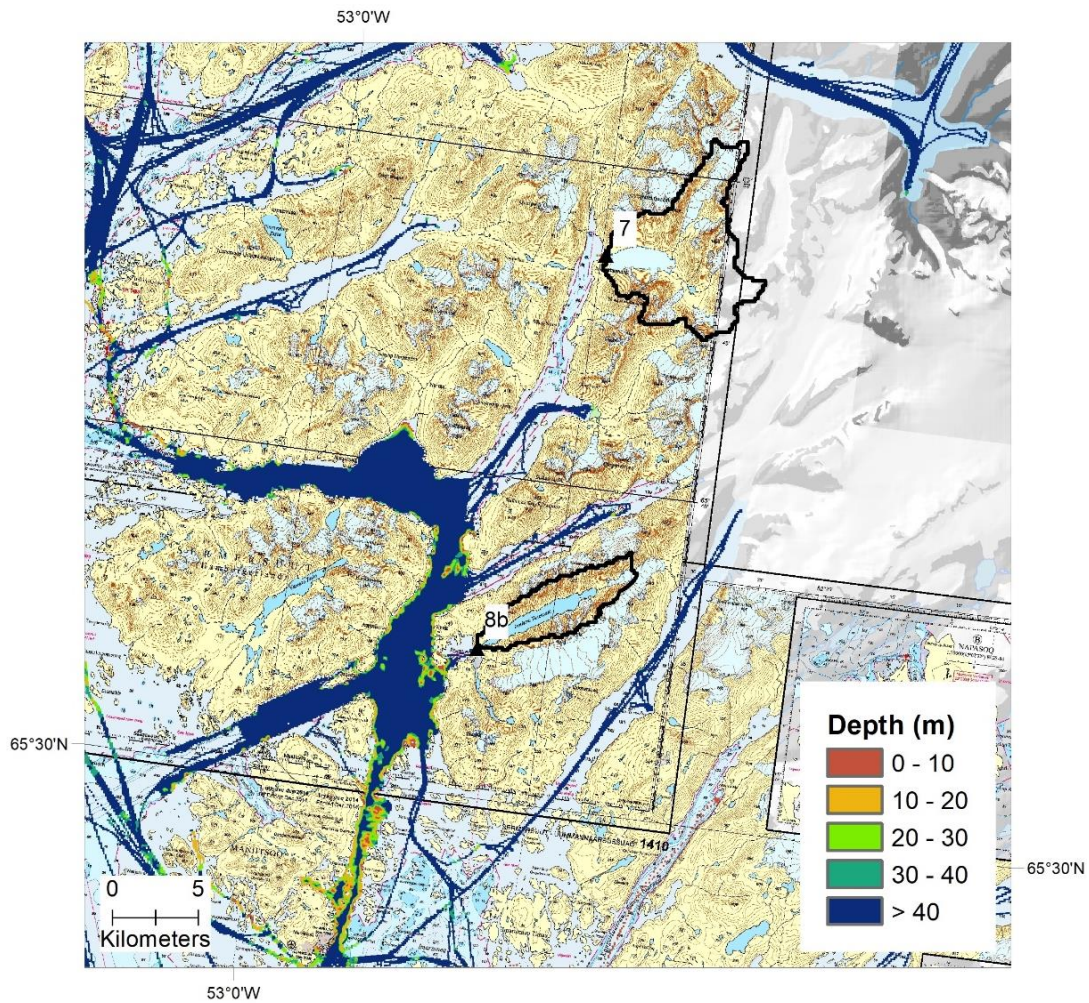


Figure 3. Map showing the delineation of the upstream catchment (as a black line) of L-07 (outlet marked "7") and L-08b (outlet marked "8"). The colour scale indicates approx. water depth from three different sources of data described in detail the text. The catchment delineation method is presented in a subsequent section. Depth relates to the minimum water depth within 100 m x 100 m grid cells.

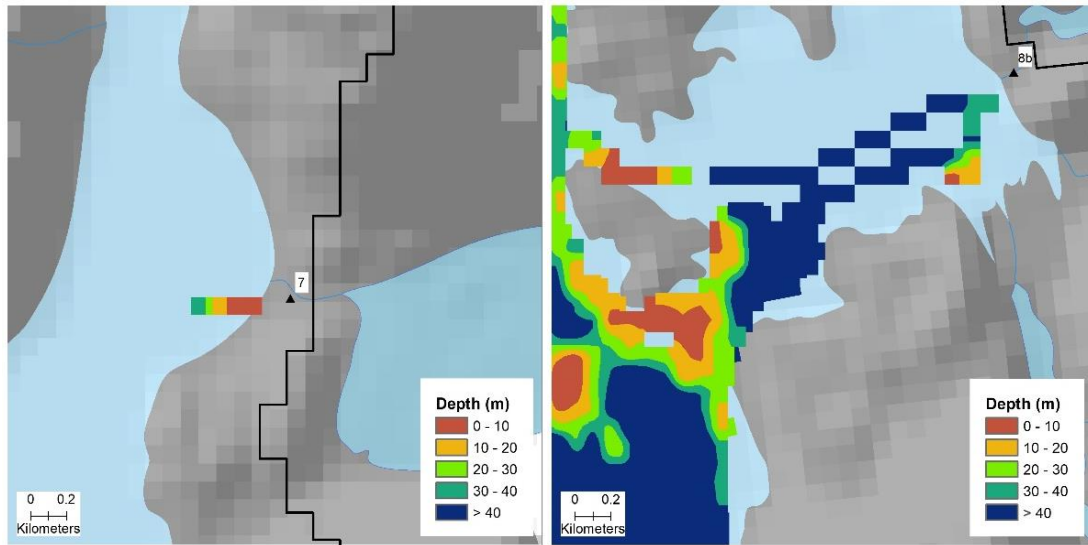


Figure 4. Close-up of the observed water depth near the shoreline of the locations L-07 (left panel) and L-08b (right panel). Depth relates to the minimum water depth within 100 m x 100 m grid cells.

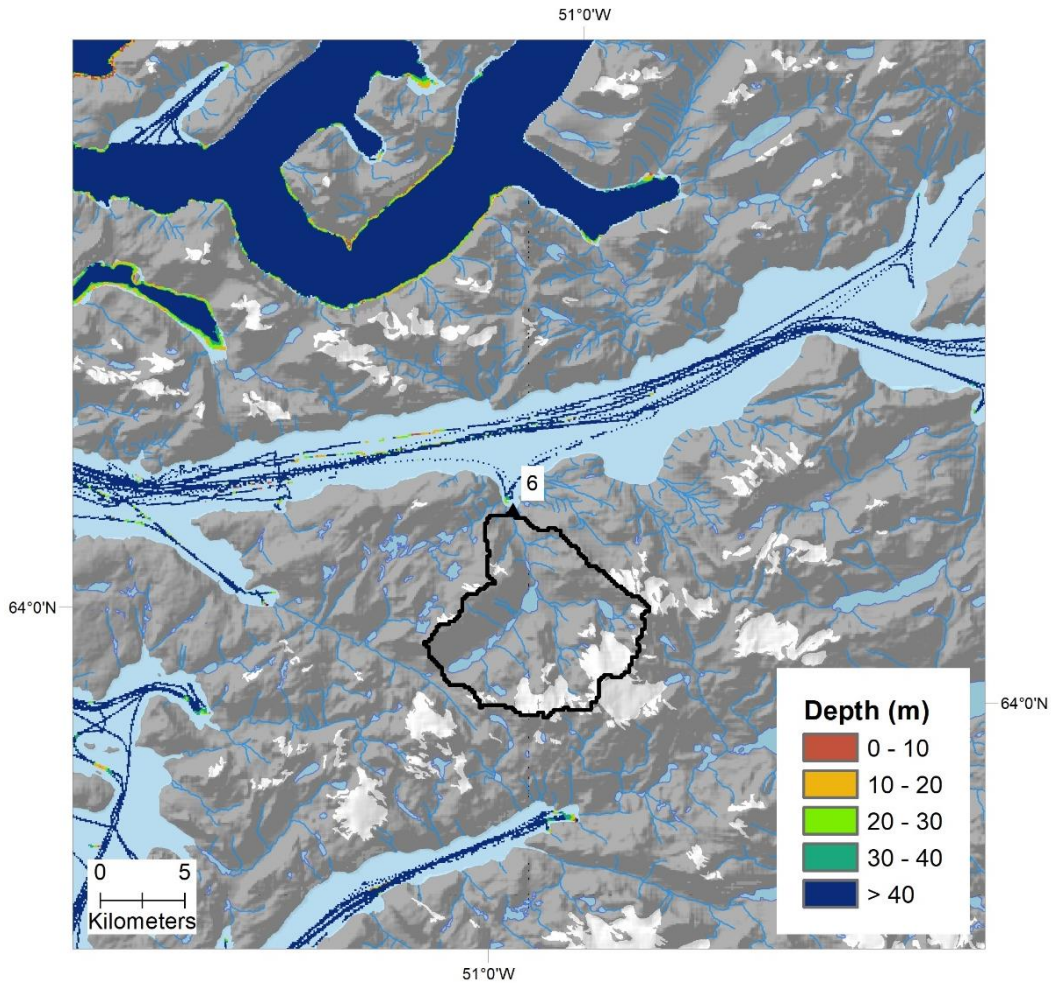


Figure 5. Map showing the delineation of the upstream catchment (as a black line) of L-06 (outlet marked "6"). The colour scale indicates approx. water depth from three different sources of data described in detail the text. The catchment delineation method is presented in a subsequent section. Depth relates to the minimum water depth within 100 m x 100 m grid cells.

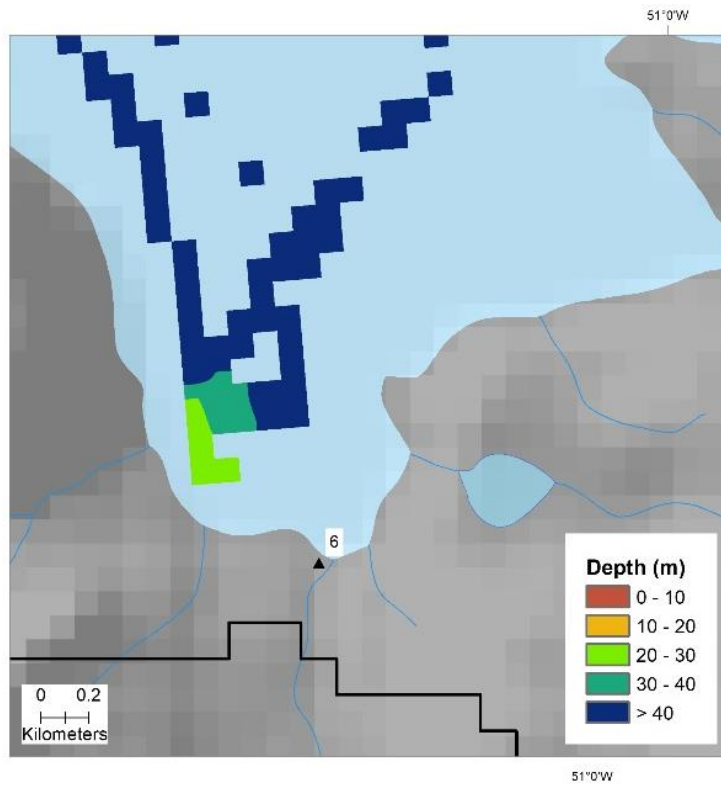


Figure 6. Close-up of the observed water depth near the shoreline of the location L-06. Depth relates to the minimum water depth within 100 m x 100 m grid cells.

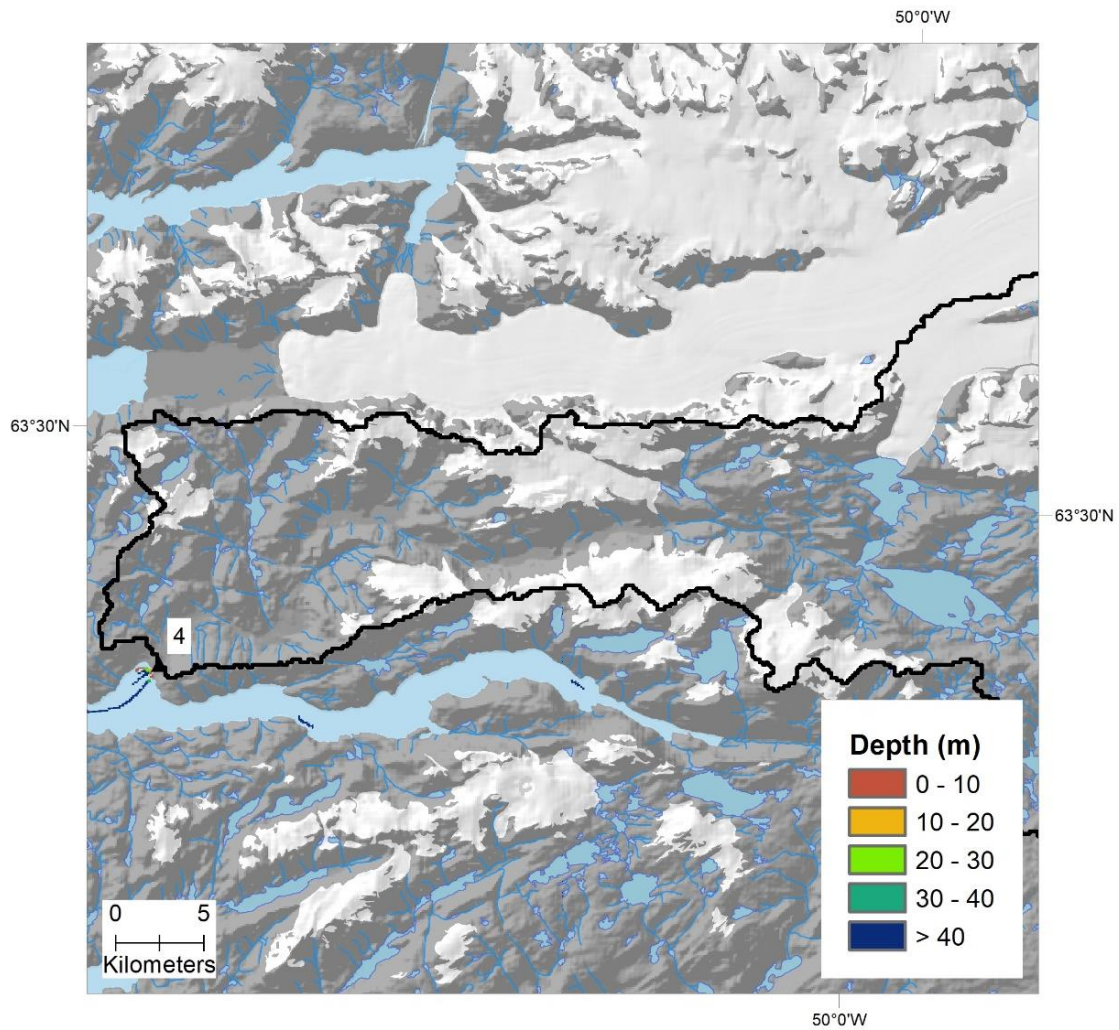


Figure 7. Map showing the lower part of the delineation of the upstream catchment (as a black line) of L-04 (outlet marked "4"). The colour scale indicates approx. water depth from three different sources of data described in detail the text. The catchment delineation method is presented in a subsequent section. Depth relates to the minimum water depth within 100 m x 100 m grid cells.

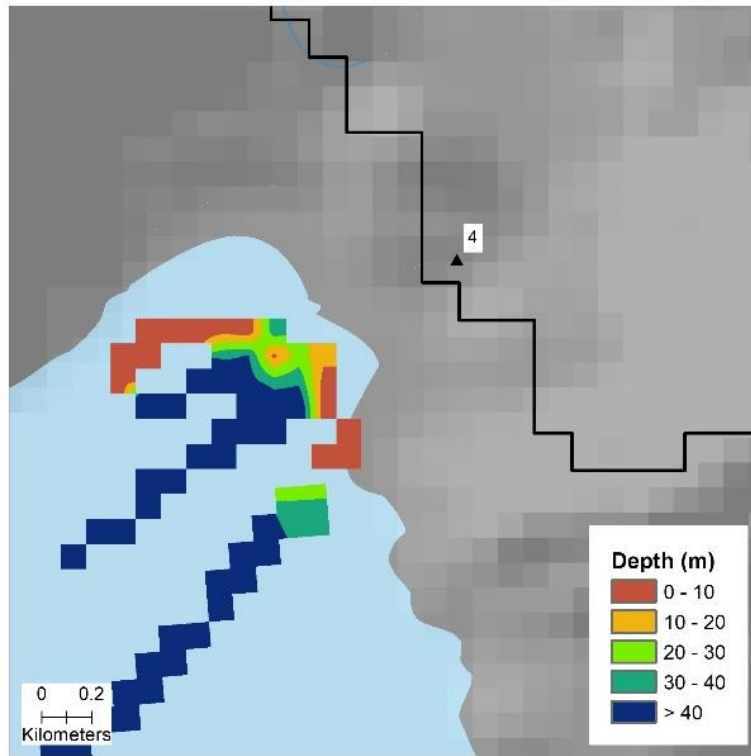


Figure 8. Close-up of the observed water depth near the shoreline of the location L-04. Depth relates to the minimum water depth within 100 m x 100 m grid cells.

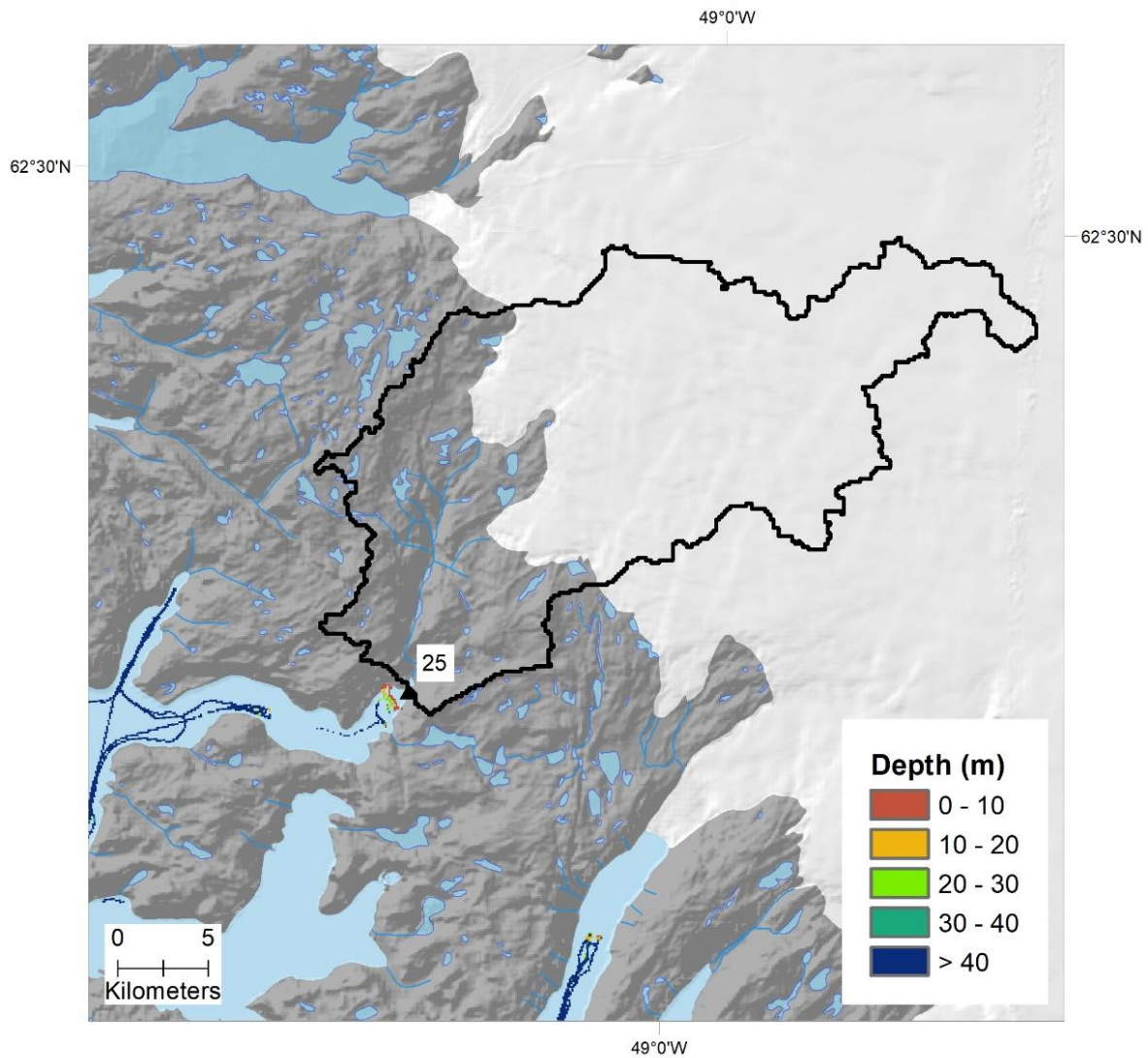


Figure 9. Map showing the delineation of the upstream catchment (as a black line) of L-25 (outlet marked "25"). The colour scale indicates approx. water depth from three different sources of data described in detail the text. The catchment delineation method is presented in a subsequent section. Depth relates to the minimum water depth within 100 m x 100 m grid cells.

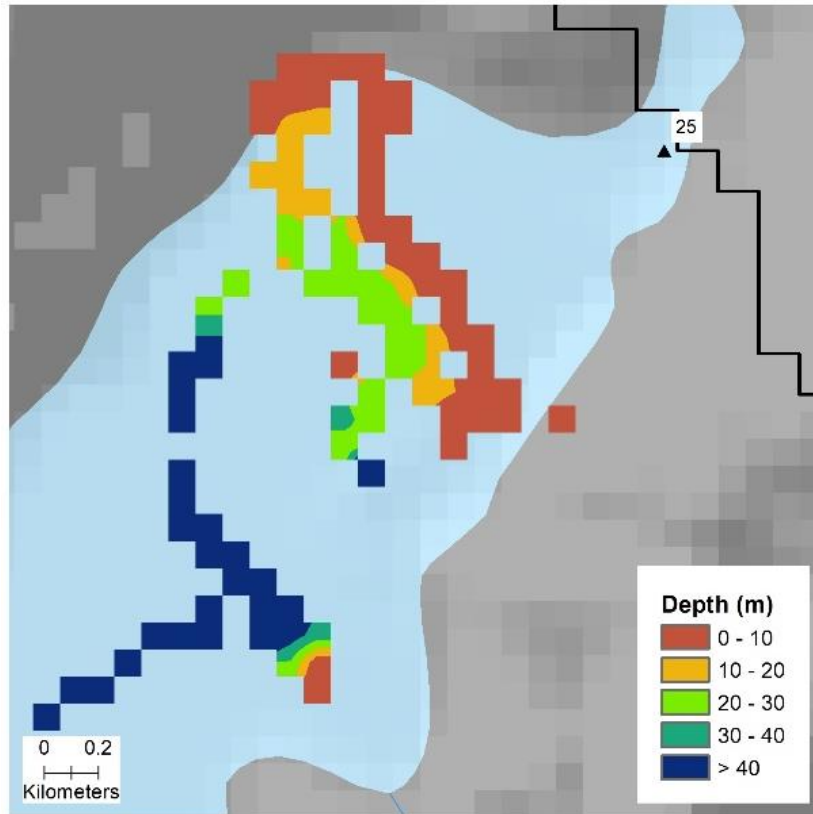


Figure 10. Close-up of the observed water depth near the shoreline of the location L-25. Depth relates to the minimum water depth within 100 m x 100 m grid cells.

5. Glaciological analysis

5.1 Catchment delineation and change risk assessment

Delineating hydrological catchments in ice-covered regions is complicated by the drainage system of the ice, which is both internal and at the base of the ice, and further changes character throughout the season. For this assessment, we have employed a simplified approach in which the drainage system of the ice is assumed to be filled up with meltwater, maximising the water pressure at the glacier base. By making this assumption, we also avoid the challenge posed by the lack of ice thickness data in the ice-marginal zone as only surface elevation data is needed.

The surface elevation is described using a digital elevation model (DEM), where available data is homogenized to a common fixed grid (a raster map) and each grid cell (square) is assigned a certain elevation. Here we have made use of dataset named 'BedMachine' (Morlighem et al., 2015), available from the National Snow and Ice Data Centre (NSIDC), which has a grid cell size of 150 m and is based on an even finer meshed (30 m) DEM named 'GIMP' (Howat et al., 2014). Choosing the slightly coarser 'BedMachine' DEM implies a 25 times reduction of computational time in the hydrological analysis.

Delineation was carried out in QGIS using the programming tool TauDEM (Terrain Analysis Using Digital Elevation Models) developed by Utah State University for extraction and analysis of hydrological information from topography, represented by a DEM.

A variety of different methods for delineation of hydrological catchments are available and we have in TauDEM chosen the method 'D-infinity Upslope Dependence', which quantifies the amount each grid cell in the domain contributes to a destination set of grid cells. The flow direction in D-Infinity proportion flow from each grid cell between multiple downslope grid cells. Following this flow field downslope the amount of flow originating at each grid cell that reaches the destination zone is defined. Upslope influence is evaluated using a downslope recursion, examining grid cells downslope from each grid cell, so that the map produced identifies the area upslope where flow through the destination zone originates, or the area it depends on, for its flow (see Fig. 11). This means that within a delineated catchment, each grid cell will contribute with a fraction between 0 and 1.

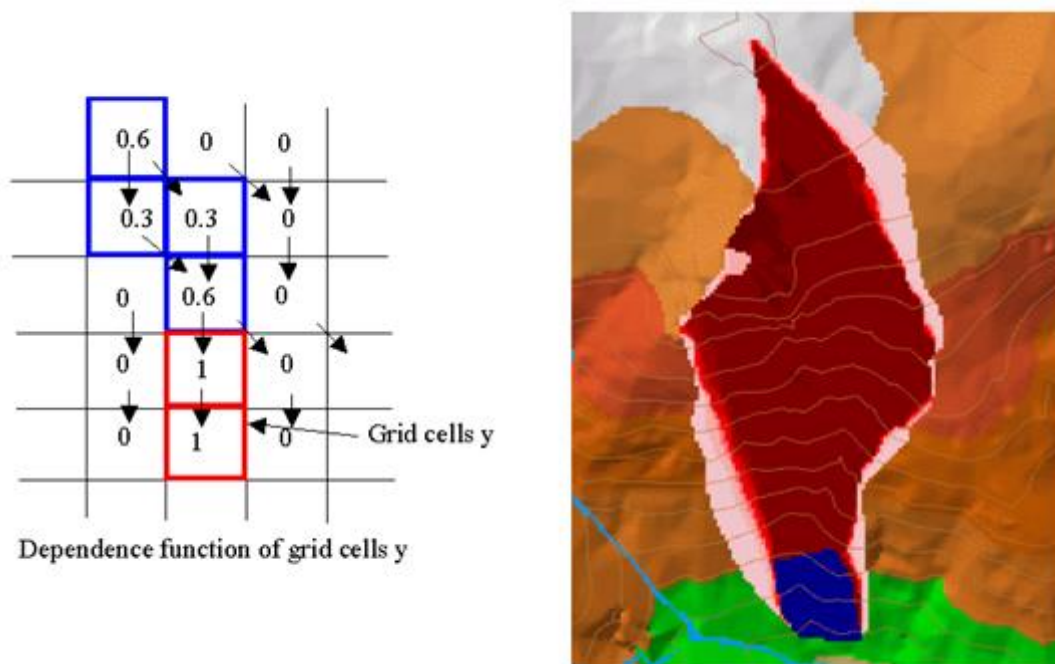


Figure 11. Illustration of the contribution from each source grid cell in the blue region x to the destination point or zone y . Source: TauDEM online documentation.

For some catchments, specifically the extensive catchments on the Greenland Ice Sheet, the contribution to runoff from a large region may actually be minor. This also indicates an increased sensitivity to changes in the size of the catchment and thus the annual runoff passing through the catchment outlet. The locations selected have, among other parameters, been classified according to the risk of catchment variability as determined from the certainty of the D-infinity delineation of the catchment. The classification also includes catchment size and estimated runoff as parameters in the classification shown in Table 2.

Parameter	L-25	L-04	L-06	L-07	L-08b
Catchment variability risk classification	2	1	4	4	4

Table 2. The catchment variability classification: (5) Small catchment with considerable risk of catchment change, (4) Small catchment with some risk of catchment change, (3) Large catchment with risk of catchment change, (2) Large catchment with low risk of catchment change over the glaciated part, (1) Very large catchment on the Greenland Ice Sheet (risk of catchment change inconsequential).

5.2 Risk assessment of glacial lake outburst floods

A common feature of catchments adjoining the Greenland Ice Sheet is glacial lake outburst floods (GLOFs), which occur when a water volume stored in an ice-dammed- or moraine-dammed lake becomes sufficient to lift the ice barrier blocking its path downstream or if the barrier is breached. Some GLOFs are known to take place from the same ice-dammed lake

every few years as the lake fills up sufficiently to break through. However, the frequency of these events is changing as the ice bodies blocking the lakes are generally thinning due to a warming climate. Thus, previous knowledge may turn out to be outdated and a known GLOF-prone lake system may pose a risk to anything and anyone downstream. To accommodate this, we have assessed the risk of GLOFs at the selected locations as listed in Table 3. The assigned risk level was a factor in the ranking of the locations.

Location	Risk level	Comment
L-04	3	A few ice dammed lakes exist within this large catchment, and new ones will probably form as the ice retreats. Supraglacial lakes can also be seen on satellite imagery, with the potential of draining rapidly. Several lakes along the Kuussuaq river may act as buffers and thereby can be expected to smooth GLOF floods. Geomorphological evidence suggests glacier surges may occur in this catchment, with the potential of damming the Kuussuaq river or other smaller rivers
L-06	1	No lake currently posing a GLOF risk
L-07	1	No lake currently posing a GLOF risk
L-08b	1	No lake currently posing a GLOF risk
L-25	2	Several lakes exist in close proximity with the ice margin. This sector of the ice margin is retreating rapidly, and new lakes may form within a few years

Table 3. *Glacial lake outburst flood (GLOF) risk level: (5) Clear indications of past glacial lake outburst floods from lakes, (4) Glacial lake outburst flood is likely, (3) Lake adjoining ice margin, but outburst flood less likely, (2) Outburst flood not so likely, but minor lake at the ice margin, (1) No lakes by ice margin.*

5.3 Runoff from meltwater and precipitation

To give the best possible estimate of the runoff from the selected catchments, we utilized a regional climate model run performed by the Danish Meteorological Institute (DMI). In this model run, catchments of sufficient size have been partitioned in ice-free and ice-covered sub-catchments. For these catchments we determined the difference between the periods 1980-1991 and 2003-2014 to evaluate the change in runoff over time.

Specifically, the runoff was estimated using 6-hourly output from the HIRHAM5 regional climate model, developed by the Danish Meteorological Institute and the Potsdam Research Unit of the Alfred Wegener Institute Foundation for Polar and Marine Research. HIRHAM5 was run with the ERA-Interim reanalysis dataset (Dee et al., 2011) as input at the domain boundaries from 1980-2014 at a 5.5 km resolution (Lucas-Picher et al., 2012). The HIRHAM5 regional climate model combines the dynamics of the HIRLAM weather forecast model (Eerola, 2006) with the physical parameterization schemes of the ECHAM

climate model (Roeckner et al., 2003). In the current configuration, HIRHAM5 is run over a Greenland-wide domain at 5.5-km resolution with six hourly inputs of horizontal wind vectors, temperature, and specific humidity from the ERA-Interim reanalysis dataset (Dee et al., 2011), supplied at the domain boundaries at all atmospheric levels to compute the atmospheric circulation within the domain at 90 s time steps. The model was run over the period 1979-2014, but surface runoff data from the first year was discarded as land surface module spin up. HIRHAM5 which is an atmosphere model was coupled to a ground model, which determines how much of the calculated melt that ends up at discharge. Model details are provided in Langen et al. (2017).

To illustrate the development of the runoff from the Greenland Ice Sheet and surrounding ice caps and glaciers over the last 35 years, we have chosen to split the climate model run 1980-2014 into two reference periods of each 11 years. The first time period is 1980-1991 and the second time period is 2003-2014. We have derived the annual mean values for the runoff from both periods, and differentiated between the ice sheet proper (Table 4) and the ice-free region including local glaciers and ice caps (Table 5). The sum of the values from Table 4 and Table 5 are given in Table 6.

Ice sheet part			
Catchment ID	Catchment area (km²)	1980-1991 annual mean runoff (Gt)	2003-2014 annual mean runoff (Gt)
4	5674	2.57	3.87
6	0	N/A	N/A
7	0	N/A	N/A
8	0	N/A	N/A
25	275	0.64	0.85

Table 4. *Modelled annual mean runoff for the ice sheet part of the selected catchments. N/A indicates that the catchment is too small to be captured by the spatial resolution of the model.*

Ice-free part, incl. local glaciers and ice caps			
Catchment ID	Catchment area (km²)	1980-1991 annual mean runoff (Gt)	2003-2014 annual mean runoff (Gt)
4	700	0.20	0.29
6	50	N/A	N/A
7	25	N/A	N/A
8	25	N/A	N/A
25	125	0.04	0.04

Table 5. *Modelled annual mean runoff for the ice-free part, incl. local glaciers and ice caps, of the selected catchments. N/A indicates that the*

catchment is too small to be captured by the spatial resolution of the model.

Catchment ID	Catchment area (km ²)	Total catchment	
		1980-1991 annual mean runoff (Gt)	2003-2014 annual mean runoff (Gt)
4	6374	2.77	4.16
6	50	N/A	N/A
7	25	N/A	N/A
8	25	N/A	N/A
25	400	0.68	0.89

Table 6. *Modelled annual mean runoff for the selected catchments, summing up the parts given in Table 4 and 5. N/A indicates that the catchment is too small to be captured by the spatial resolution of the model.*

The difference in runoff between the two periods are due to changes in weather and climate conditions. Generally, the majority of the melt occurs near the ice margin (the ablation zone), whereas the accumulation takes place in the more central parts of the ice sheet. The model results show that the two analyzed catchments experience an increase in the mean annual meltwater runoff from the first period to the second period (Fig. 12). Furthermore, the largest change is seen in the summertime (June-August), although large relative differences are seen in May, September and October, mainly in West and Southwest Greenland (monthly differences not shown on Greenland scale). The largest differences occur in the summer in the ablation zone with West and Northwest Greenland. The relative differences (in %) are visible far up on the ice sheet, as certain parts, which just 30 years ago only experienced little melt, now melts at an increasing rate. The general increase in ice sheet runoff from the model is a direct consequence of the larger amount of energy received from an increasingly warmer climate.

The ice-free regions generally experiences a decrease in precipitation, which has the consequence that less water is available for catchments (Fig. 13). However, exceptions are found in Southwest Greenland. The amount of freshwater from precipitation over the ice-free regions is much smaller than the ice sheet meltwater runoff. A comparison between Figs. 12 and 13 shows that the change in discharge in some places reach two orders of magnitude larger in the ice-free region. The general picture is a difference of one order of magnitude, if comparing individual catchments (Table 4 and 5).

Some of the selected catchments are too small to be properly resolved in the regional climate model and thus do not provide meaningful results. For these cases, the catchment areas are marked with N/A in Table 4 and 5. While downscaling methods have been developed to evaluate such contributions (e.g. Noël et al., 2016), they generally depend on in situ observations within the catchment to reduce the inherent uncertainties of the approach. We have illustrated the evolution in runoff for the two catchments, L-04 and L-25, which are

large enough to be captured by the spatial resolution of the model, on a monthly basis in Figs. 14 and 15.

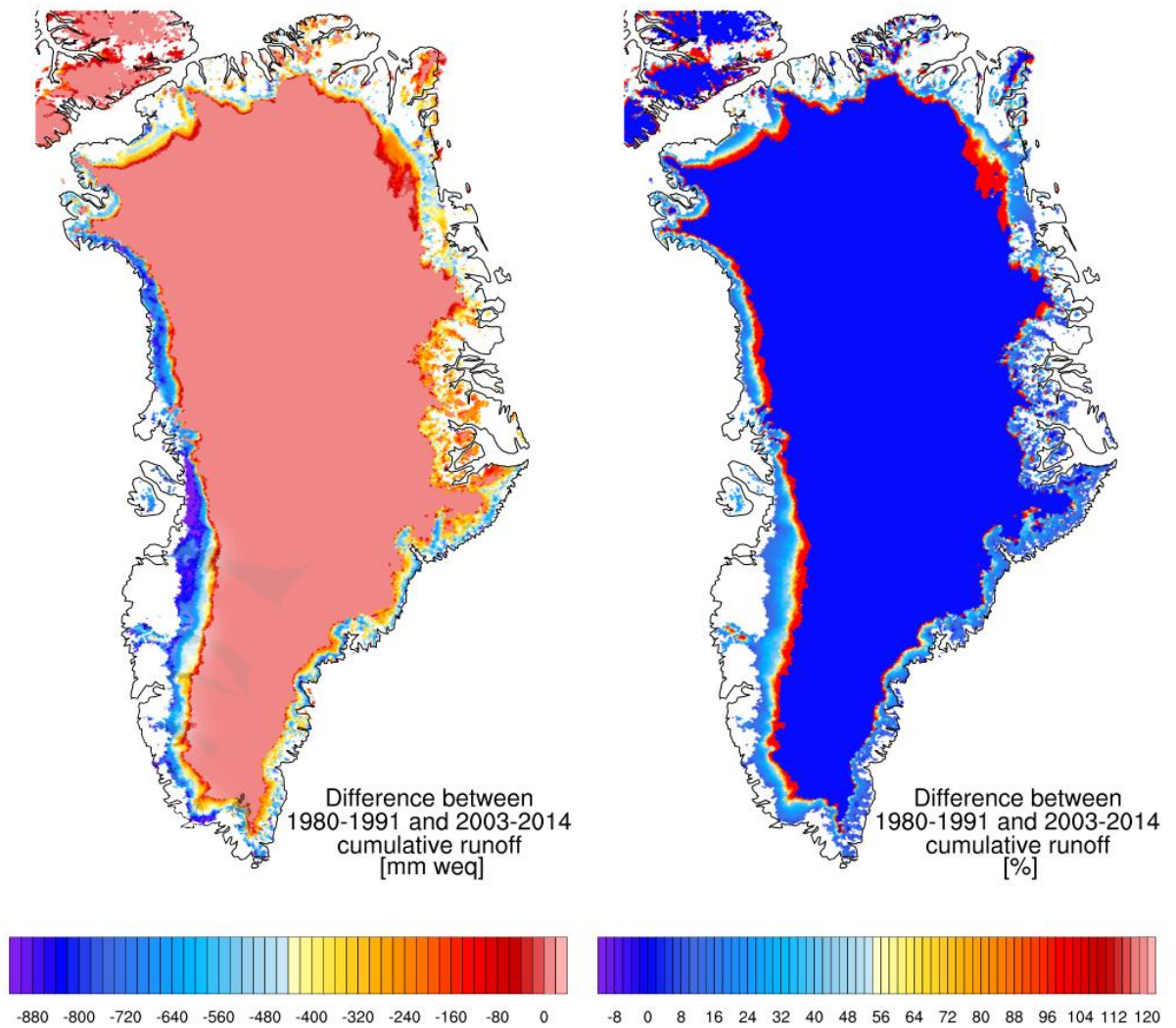


Figure 12. Temporal evolution of the modelled ice sheet runoff between 1980-1991 and 2003-2014, illustrated as an absolute difference in mm water equivalent [mm weq] (left panel) and as relative difference given in percent [%] (right panel), respectively.

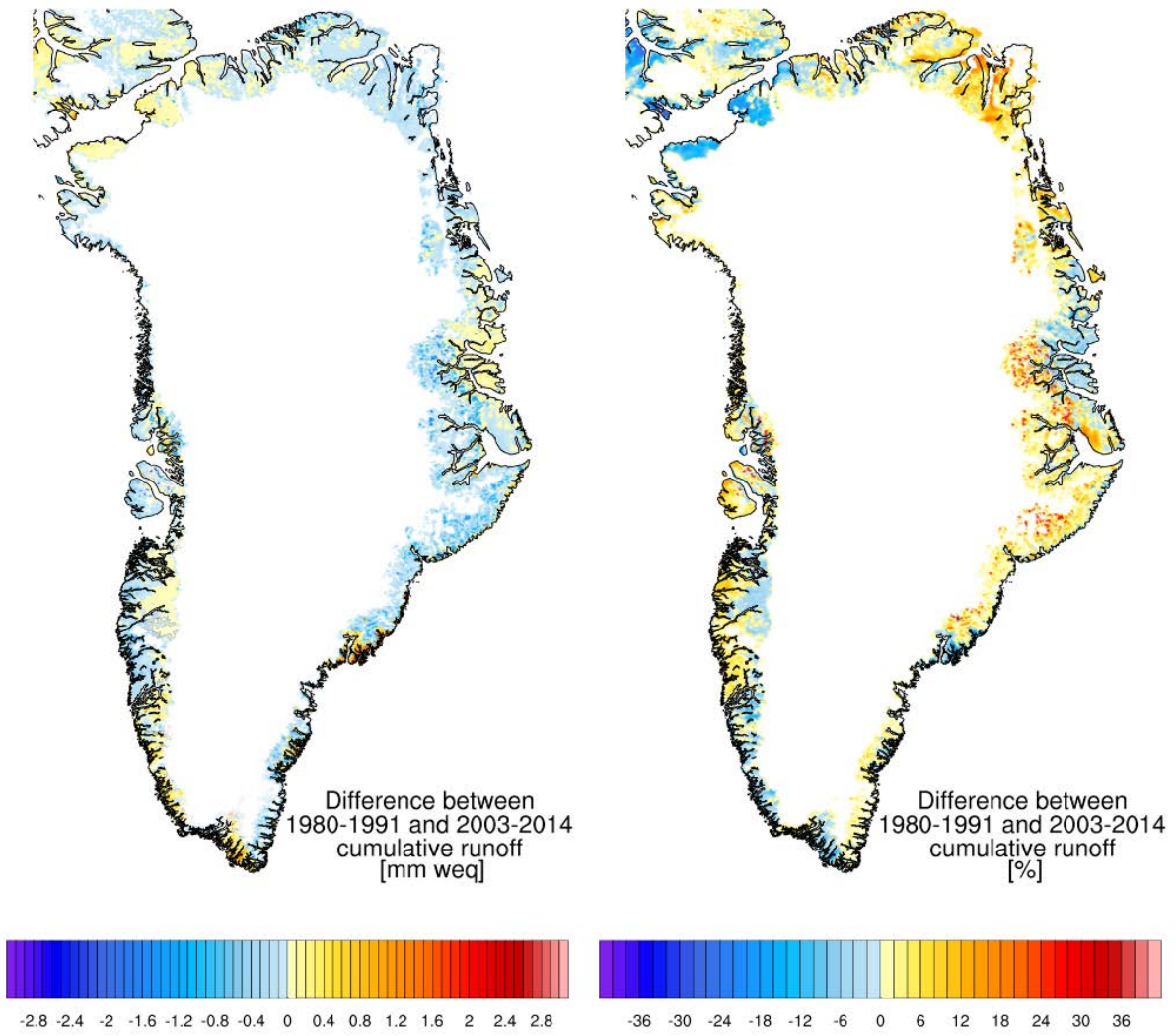


Figure 13. Temporal evolution of the modelled runoff from the ice-free region between 1980-1991 and 2003-2014, illustrated as an absolute difference in mm water equivalent [mm weq] (left panel) and as relative difference given in percent [%] (right panel), respectively.

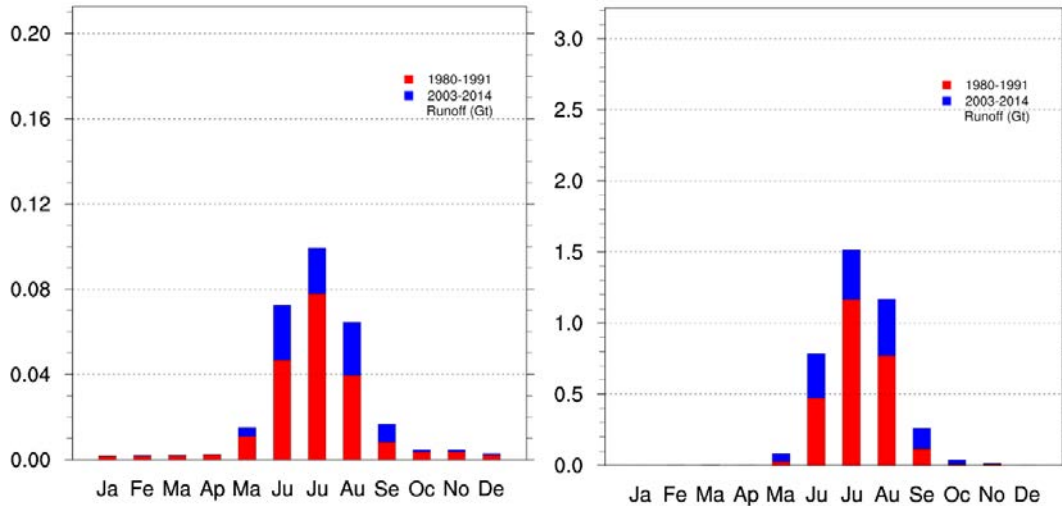


Figure 14. *Left panel: the monthly evolution in runoff for the ice-free (incl. local glaciers and ice caps) part of the L-04 catchment. Right panel: the monthly evolution in runoff for the ice sheet part of the L-04 catchment. Both histograms are cumulative, implying that the blue bar should be added to the red bar to get the value for the latter period 2003-2014. Note that the scale on the y-axes differ.*

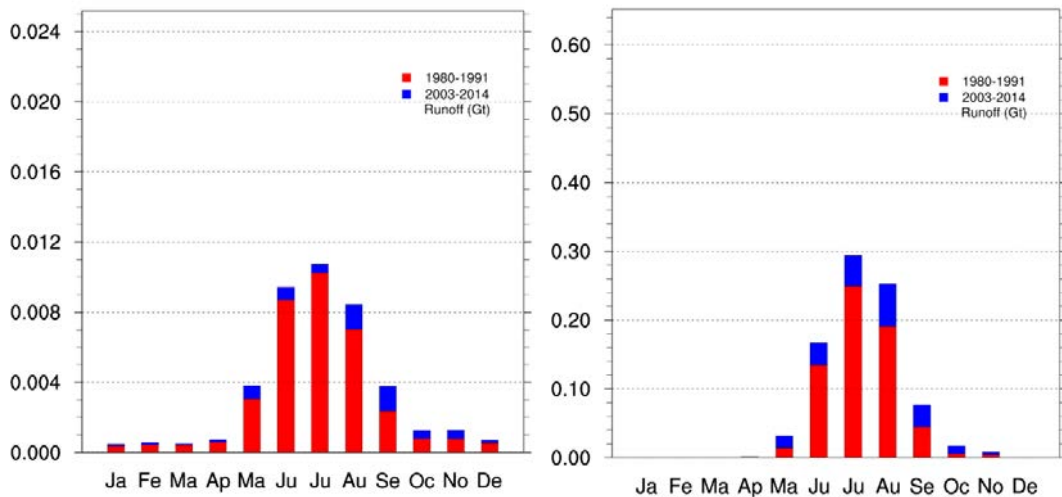


Figure 15. *Left panel: the monthly evolution in runoff for the ice-free (incl. local glaciers and ice caps) part of the L-25 catchment. Right panel: the monthly evolution in runoff for the ice sheet part of the L-25 catchment. Both histograms are cumulative, implying that the blue bar should be added to the red bar to get the value for the latter period 2003-2014. Note that the scale on the y-axes differ.*

5.4 Estimation of the age of the meltwater source ice

A significant part of the discharge consists of ice sheet or glacier meltwater. The age of the source ice for this meltwater can be many thousands of years and depends partly on local

conditions, but is generally governed by upstream conditions. The left part of Fig. 16 shows a cross section of an ice sheet, from surface to bedrock. Two trajectories mark possible particle paths through the ice sheet for an ice crystal, originally falling as snow, depending on where it originates on the ice surface. It illustrates that the higher on the ice sheet the snow fell in the accumulation zone, the deeper the trajectory of the ice crystal, and subsequently, the closer to the ice margin the reappearance in the ablation zone. The accumulation zone is the only region on an ice sheet or glacier, where the mass balance is positive, i.e. more snow is deposited than what melts or blows away, whereas the opposite is true in the ablation zone, where the mass balance is negative, i.e. more mass is removed than added. This implies that layer after layer of snow is buried in the accumulation zone every year, while in the ablation zone they reappear. If there was no melting at the bottom of the ice sheet and layers never folded, it would in principle be possible to make 'horizontal' ice cores along the surface of the ice margin, with the oldest ice closest to the margin as illustrated in the right side of Fig. 16. The age of the ice at the margin is thus determined by the distance and pace of the ice movement towards the margin. Under the right circumstances, it is therefore possible to find extremely old ice at the ice sheet margin, as shown in e.g. Reeh et al. (2002).

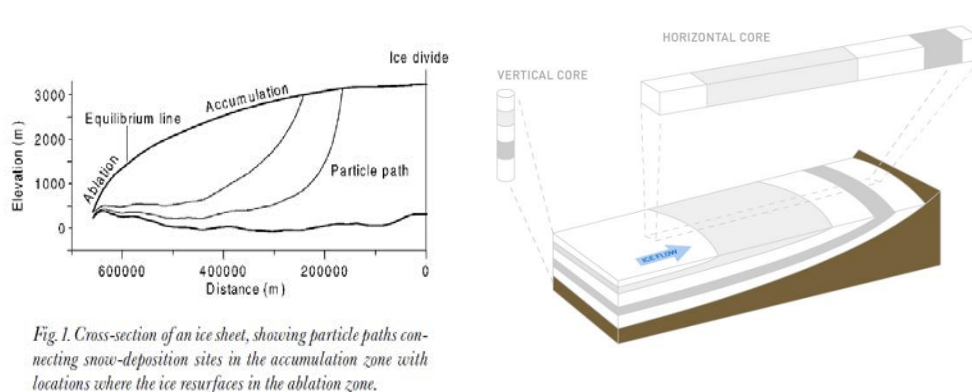


Fig. 1. Cross-section of an ice sheet, showing particle paths connecting snow-deposition sites in the accumulation zone with locations where the ice resurfaces in the ablation zone.

Figure 16. Two figures, illustrating why old ice can be expected at the ice sheet margin. Left: Reeh et al. (2002). Right: figure from www.niwa.co.nz.

5.4.1 Ice-dynamic model setup

To estimate the age of the ice at various locations around the ice margin (left panel of Fig. 17), we have employed the ice-dynamic model PISM (Parallel Ice Sheet Model), which is a three-dimensional, thermo-mechanical coupled model (Bueler and Brown, 2009; Winkelmann et al., 2011; Aschwanden et al., 2012). The model is developed at the University of Alaska and the Potsdam Institute for Climate Impact Research. PISM makes use of a simplified description of ice-dynamics, combining the so-called 'shallow-ice' and 'shallow-shelf' approximations, which makes it possible to study the flow of large ice masses like the Greenland Ice Sheet, over long time scales (tens of thousands of years), as those of interest here. The model has an 'age-tracking' method, thereby keeping track of the age of the ice, a method we employ to estimate the age of the ice at the margin.

As input to the model, we have used present-day topography, forced with present-day climate (surface mass balance as shown in the right panel of Fig. 17, and air temperature).

The model covers the entire Greenland Ice Sheet with a spatial resolution of 10 km. All model experiments have been conducted over a 100,000 year period of constant climate, reaching a steady state during this time. Additionally, model experiments at 20 km spatial resolution with only the 'shallow ice' approximation have been conducted to test the robustness of the results. These sensitivity model runs show the same results as the main model experiments on the scale examined here.

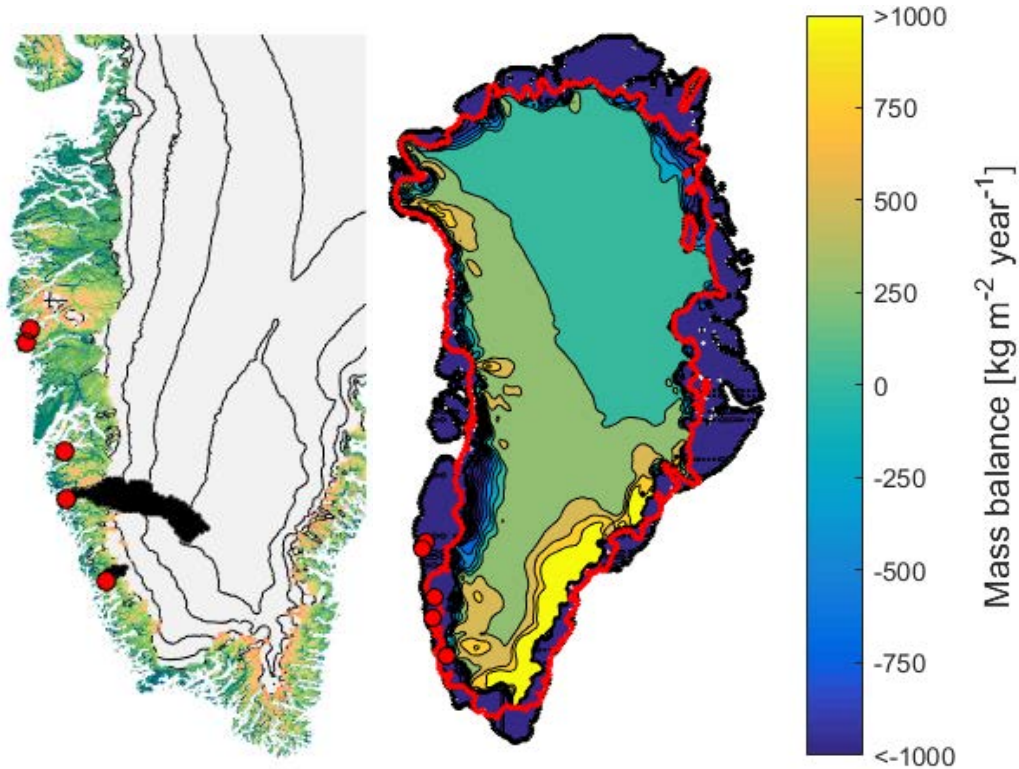


Figure 17. *Left panel: selected locations (red circles) with their respective catchments in black. Right panel: present-day surface mass balance from Ettema et al. (2009). The heavy red line indicates the extent of the ice in the model. The black line separates land/ice from ocean. The region between the red and the black line is thus ice-free land in the model.*

Not all locations receive meltwater from the ice sheet, but rather from local glaciers and ice caps. These are not included in the large-scale model experiments described here. Blue colours in Fig. 17, right panel, shows regions with net melting, while yellow/green colours shows the accumulation zone. As Fig. 17 illustrates, the ablation zone is generally quite narrow, but widens in some regions, like western Greenland, where it is more likely to find ancient ice at the surface due to the long distance to the ice divide and a broad ablation zone to drag out the ice layers from below. On the other hand, in southern Greenland, it should be expected that the ice at the margin is typically younger and that the older ice resurfaces in a more narrow region, as the distance to the ice divide is short, the accumulation rate is high, and the ablation zone is narrow.

5.4.2 Estimated age of the ice

Upon reaching a steady state during the 100,000 year model run, the ice sheet turns out to have a somewhat larger extent and volume than the actual present-day Greenland Ice Sheet. Some locations in South Greenland situated in the ice-free sector is covered by ice at the end of the model run (compare for example the ice sheet extent in South Greenland between Fig. 17 (right panel) and Fig. 18). This is a consequence of using present-day climate to force the model as the ice sheet of the present is not in balance with present-day climate, as well as the choice of 10 km spatial resolution. More detail would be included if running the model at higher spatial resolution, both with respect to the surface mass balance, where it may play an important role due to the narrow ablation zone, and in relation to the basal topography, where smaller outlet glaciers would become apparent. However, a higher spatial resolution prohibitively increases the computational cost and has not been possible within the framework of this investigation. Still, the model setup does an excellent job at estimating the age of the ice.

While the model experiments have been conducted prescribing a 100,000 years of constant climate, the climate has of course not been constant over this period. During the last ice age, which terminated around 11,700 years ago, it was of course much colder than today and accumulation was around half of the present-day value. These conditions influence the flow of the ice and has an impact on the estimation of the age of the ice. For this reason we restrict ourselves to partition the selected locations into either ice-age ice (i.e. generally older than 11,000 years) or the younger Holocene ice (Holocene: Geological era covering 11,700 years ago to present).

The modelled age of the ice appearing on the surface is shown in Fig. 18, while Fig. 19 shows two examples of cross sections, where layers of various age can be traced in the ice sheet.

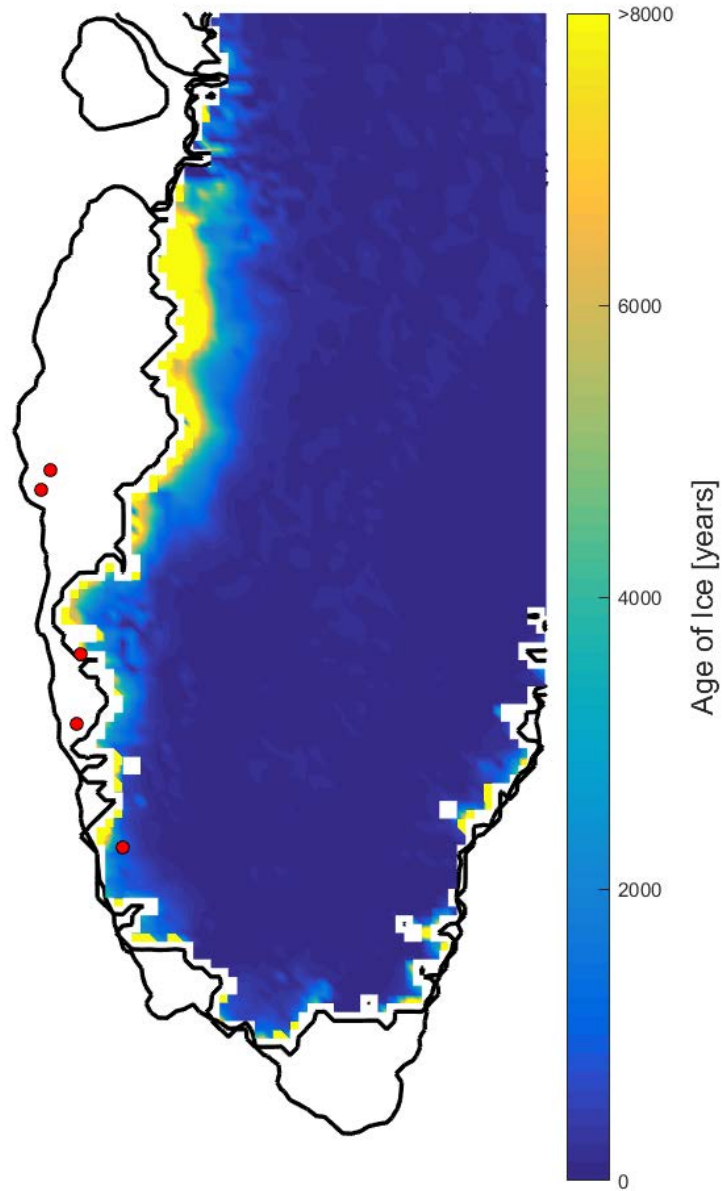


Figure 18. *Model result: age of the ice at the surface at the conclusion of the model run.*

In the region with the broad yellow ablation zone in Fig. 18, the age at the surface of the ice exceeds 8,000 years. However, the narrow, yellow areas/dots in the southern region are artefacts from the ice modelling in combination with the contouring method and is not a real indication of pre-Holocene ice surfacing.

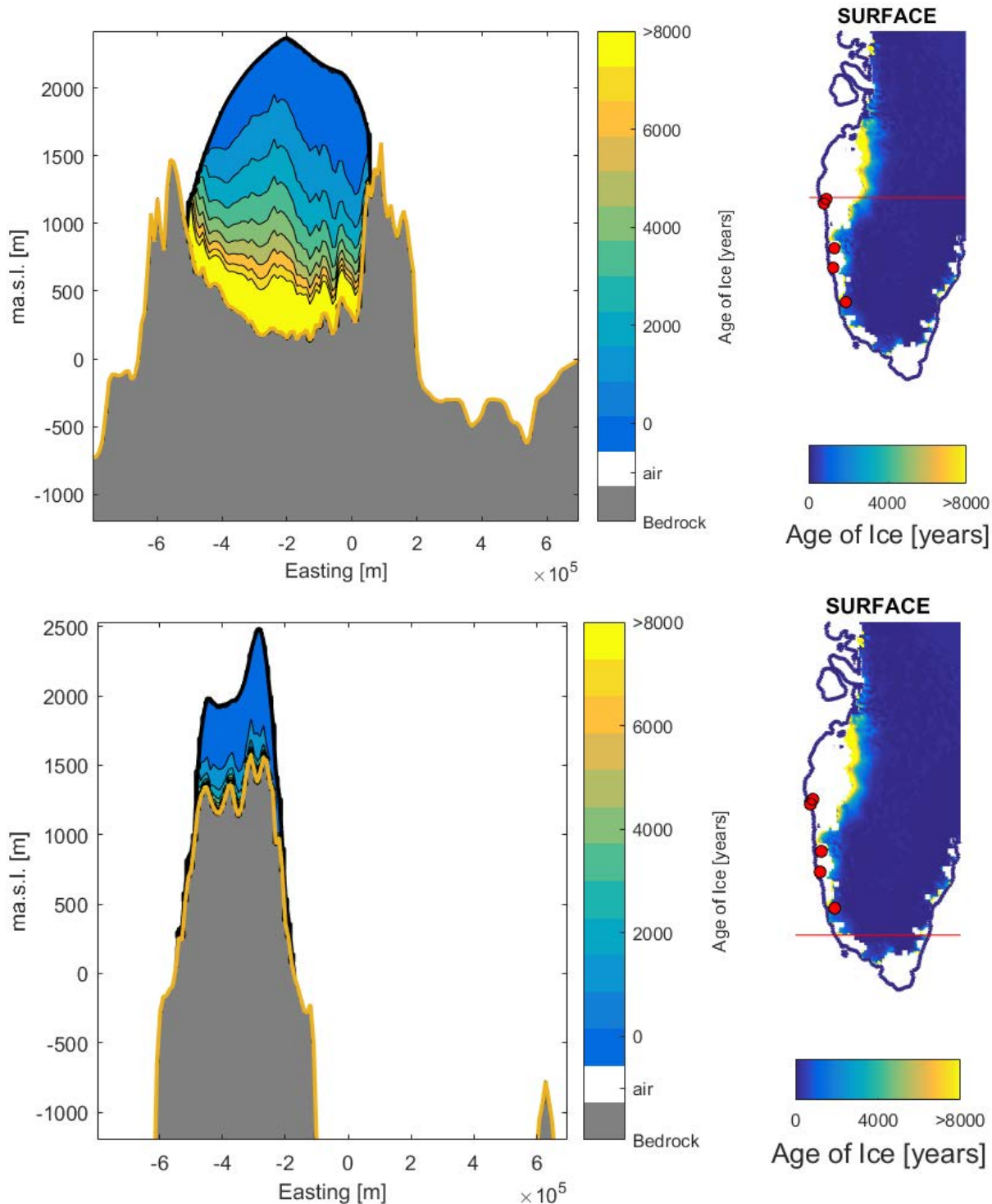


Figure 19. Top left panel: cross section of the ice sheet in southern West Greenland showing the age of the ice at depth along the thin, red line shown in top right panel. Bottom left panel: cross section of the ice sheet in the extreme South Greenland showing the age of the ice at depth along the thin, red line shown in bottom right panel. Notice the different scale of the x- and y-axis, distorting the relationship between the width and the height of the ice sheet.

Our results indicate that ice from the last ice age can be found at the surface of the ice margin in a region stretching from the Disko Bay and somewhat south of Kangerlussuaq in

southern West Greenland. This is supported by oxygen isotope measurements from a few sites in the region (Reeh et al., 2002). In South Greenland, the ice is mainly from the current Holocene period. Even though the ice extent in our simulation is larger than what is the case in reality, it is still possible to conclude that the ice is of Holocene origin. This also matches an earlier investigation by Mayer et al. (2003), which arrives at an age of the ice of 5-6,000 years at two locations in South Greenland. For the locations that do not receive meltwater from the Greenland Ice Sheet, but rather from local glaciers and ice caps, the age of the ice melted is expected to be rather young and most likely no older than the latter half of the Holocene. This conclusion is based on their more limited extent and their location in a maritime climate with more precipitation.

The somewhat coarse division in Holocene and ice age ice is a consequence of the simplified model setup. If a more specific determination of the age of ice from a particular location is desired, this can be accomplished by combining modelling of the ice dynamics of the individual ice catchment with oxygen isotope measurements of samples from the ice surface.

Location	Age	Source	From
L-04	Holocene/ice-age	Ice sheet + local glaciers	Estimate
L-06	Late Holocene	Local glaciers	Estimate
L-07	Late Holocene	Local glaciers	Estimate
L-08b	Late Holocene	Local glaciers	Estimate
L-25	Holocene	Ice sheet	Model

Table 7. *The modelled or estimated age of the ice from which the meltwater originates at the selected locations. Most locations (except L-25) are seen to be either local glaciers or small ice sheet catchments not directly resolved by the ice-dynamic model. For these locations, the age has been estimated from glaciological expertise and comparison to model results of the ice sheet proper.*

6. Results from the water quality analysis

6.1 Sampling methodology

Water samples were retrieved during a field campaign in June 2017. Water sampling was as far as possible conducted where the water was well-mixed and where no animal excrements were visible on shore (see sampling locations in Table 8). When possible, samples were taken a few metres from the shore of the river. The person sampling wore sleeve protectors as well as nitrile gloves, which were disinfected with alcohol before sampling the water.

Location	N	W
L-25	62°16.553	49°16.954
L-04	63°23.190	50°46.770
L-06	64°04.372	51°01.497
L-07	65°47.223	52°39.421
L-08b	65°34.749	52°45.246

Table 8. *GPS-coordinates for water sampling for chemical and microbiological parameters.*

Samples for bacterial counts taken in glass bottles sterilized by autoclavation, by opening them 10-20 cm below the water surface to avoid surface contamination (see Fig. 20).

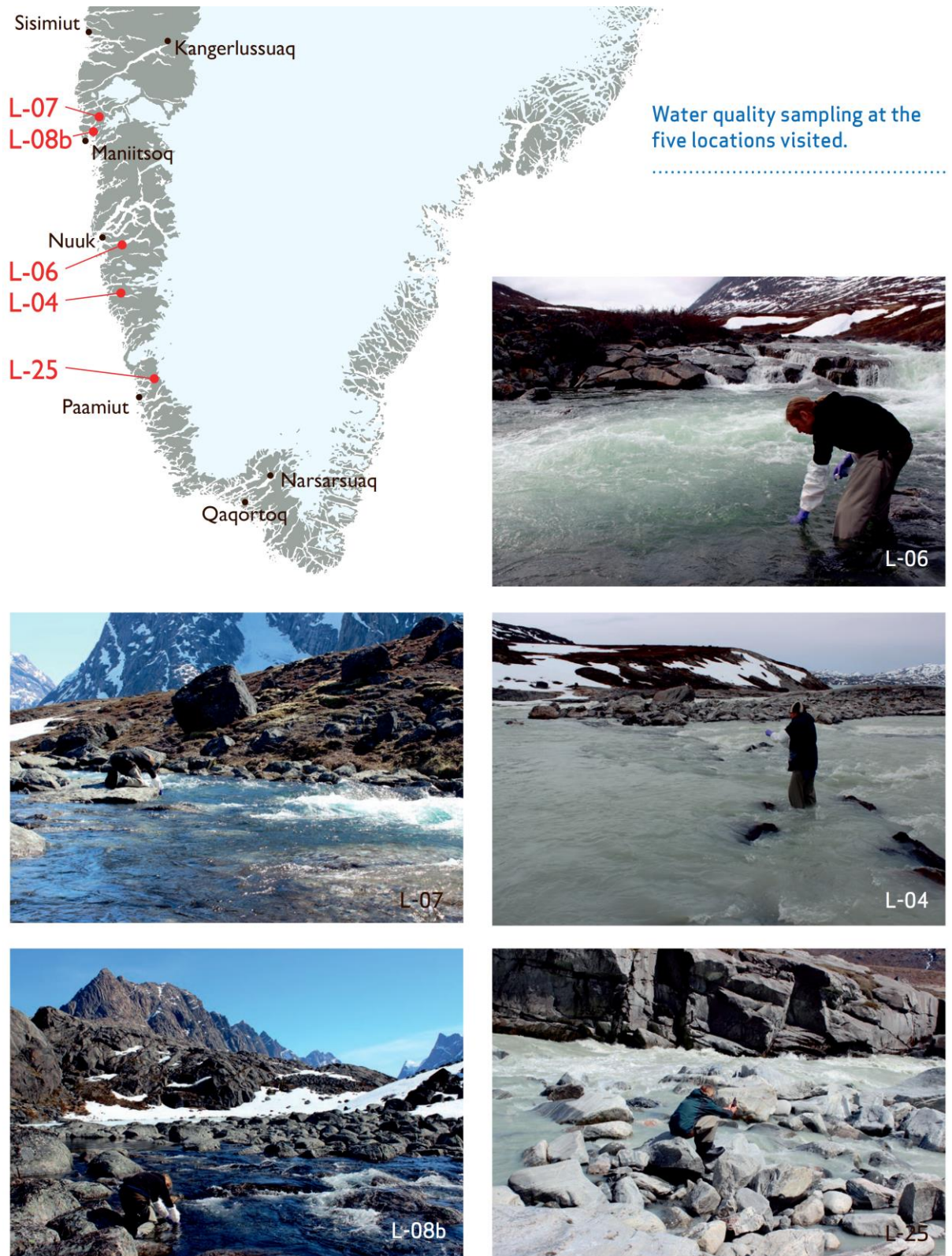


Figure 20. Water sampling at the selected locations, with inserted map. Note that the sampling of L-25 was conducted at a waterfall several kilometres upstream from where the river discharged into the fjord as there was no significant waterfall at the river mouth.

After one hour, a part of the sample was transferred from the sampling bottle to a sterile centrifuge tube. This partial sample was used for a bacterial count of an undiluted sample. Additionally, total plate count (colony-forming unit, CFU) was done on a 10x diluted sample. This diluted sample was produced using sterilized water from the same location (using a 25mm Q-max cellulose acetate 0.2µm filter from Frisenette). The transfer to various petri-films was done using sterile pipette tips, while wearing nitrile gloves disinfected with alcohol and working on a table also disinfected with alcohol onboard the ship (see Fig. 21).



Figure 21. *Temporary laboratory onboard the ship.*

Remaining samples were taken in various plastic and glass bottles depending on the sample type (see Fig. 22 and Table 9). Samples for analysis of metals, cyanobacterial toxins (microcystins and Anatoxin-A-fumarat), anions and cations were initially taken in a 1 L glass bottle, which was subsequently put aside for 1-2 hours before the contents were divided as partial samples into the final analysis bottles. For analysis of trace metals, nitric acid was added to the analysis bottle prior to use. For the microcystin-analysis, sodiumthiosulfate was added to the analysis bottle prior to use. For anions and cations, a 40 mL sample was filtered through a 25mm Q-max cellulose acetate 0.2µm filter from Frisenette and transferred to a centrifuge tube.



Figure 22. Sampling bottles from fieldwork in 2017 ready for shipment from Nuuk, Greenland. A broad variety of samples were taken to cover the spectrum of desired analysis parameters. Most analyses were conducted subsequently by commercial laboratories, with the remaining conducted onboard the ship (bacterial counts) or in GEUS laboratories (anions, cations, pH and alkalinity).

Parameter	Type of analysis	Place of analysis	Container	Comment
pH	Electrode	On-site+GEUS	n/a	
Oxygen	Electrode	On-site	n/a	
Conductivity	Electrode	On-site	n/a	
Anions ¹	Ion chromatograph	GEUS	50 mL plastic	Filtration + cooling
Cations ²	Ion chromatograph	GEUS		Filtration + cooling
Trace metals	DS/EN ISO 17294m:2016 ICP-MS	Eurofins	30 mL plastic	Acid conservation
Radioactivity	ISO 10704+13168:2015	Eurofins	250 mL plastic	
Microcystins	ISO 20179 mod. LC-MS/MS	Eurofins	100 mL glass	Added thiosulfate
Anatoxin-A-fumarat	LC-MS	Eurofins	1 L glass	
Coliform bacteria	3M Petrifilm Aqua x5	On-boat	36°C incubator 21h	Undiluted
Enterobacteriaceae	3M Petrifilm Aqua x5	On-boat	36°C incubator 21h	Undiluted
Total CFU	3M Petrifilm Aqua 2x5	On-boat	22°C incubator 68h	Undiluted + 10x
Thermotolerant CFU*	3M Petrifilm Aqua x5	On-boat	36°C incubator 44h	Undiluted

*Method developed for total CFU but adapted to thermotolerant CFU.

¹Fluoride, chloride, bromide, sulfate, nitrate, phosphate.

²Sodium, potassium, calcium, magnesium.

Table 9. Analytical program for chemical and microbiological parameters.

6.2 Inorganic parameters including selected trace metals

Results from the analyses are reported in Table 10 along with the corresponding quality requirements. With a one exception, none of the chemical parameters investigated exceed the currently applicable drinking water quality requirements in Greenland, Denmark, the EU or the USA, or for bottled water in Denmark and of the ICBWA (The International Council of Bottled Water Associations). The exception mentioned is the pH-value, which in a few cases is below the existing 6.5 threshold (7.0 in Denmark). However, this is expected from previous investigations of surface water in Greenland (Rambøll, 2006). Drinking slightly acidic water (defined here as pH 6-7) does not pose a problem in itself, and it is an option to adjust the pH-value with a base, e.g. CaCO_3 (chalk) or NaOH . Very small amounts of base would be required to do this as the water alkalinity of the relevant locations is extremely low (<0.1 , see Table 10).

The water from the locations visited have been analysed for the most usual inorganic parameters and it is thus positive that they are all within the quality requirements and in most cases well within. We cannot completely rule out that some of those metals we have not analysed for, could be present in elevated concentrations. However, we consider this to be a fairly low risk, as we have included two indicator-parameters (fluoride and nickel) in the investigation. Fluoride (F) would be elevated in connection with the alkaline intrusions in South Greenland, but values remain below the detection threshold of the analysis for all locations. Nickel may pose a problem in its own right, but may also be related to the occurrence of other undesirable metals. While the nickel concentrations at L-25 and L-04 were significant, both remained well below the threshold criterion (see Table 10). An extended analysis of trace metals may be in order at these locations two if they are chosen for exploitation. Notably, L-25 has a relatively high level of several trace metals, where cobalt and nickel reach slightly above 50% of the threshold criterion.

Parameter	Unit	L-25	L-04	L-06	L-07	L-08b	Criterion
pH _{field}	-	6.6	6.4	6.2	6.8	6.1	6.5-8.0
pH _{lab}	-	6.38	6.74	6.25	6.69	6.17	6.5-8.0
Alkalinity _{lab}	meqv/l	0.13	0.08	0.05	0.13	0.04	-
Conductivity _{field}	mS/m	15	15	13	22	15	<250
Temp _{field}	°C	3.7	4.1	4.1	2.9	1.3	-
F ⁻	mg/L	<0.04	<0.04	<0.04	<0.04	<0.04	1.5
Cl ⁻	mg/L	0.68	0.51	1.12	0.99	2.41	250
NO ₃ ⁻	mg/L	0.38	0.10	0.07	0.09	0.13	44
PO ₄ ³⁻	mg/L	<0.05	<0.05	<0.05	<0.05	<0.05	-
SO ₄ ²⁻	mg/L	0.91	2.35	1.27	3.03	0.99	250
Na ⁺	mg/L	0.74	0.66	0.88	0.99	1.64	175
K ⁺	mg/L	0.82	0.65	0.42	0.38	0.15	-
Ca ²⁺	mg/L	1.44	1.50	0.88	2.11	0.53	-
Mg ²⁺	mg/L	0.25	0.21	0.20	0.65	0.26	50
Antimony (Sb)	µg/L	< 0.2	< 0.2	< 0.2	< 0.2	< 0.2	5
Arsenic (As)	µg/L	0.081	0.097	< 0.03	< 0.03	< 0.03	5
Barium (Ba)	µg/L	67	34	5.8	3.1	< 1	700
Lead (Pb)	µg/L	0.65	0.63	0.075	0.044	0.12	10
Boron (B)	µg/L	< 1	1.9	1.8	1.4	3.3	300
Cadmium (Cd)	µg/L	0.0035	< 0.003	< 0.003	< 0.003	< 0.003	3
Chromium (Cr)	µg/L	12	4.7	0.094	0.094	< 0.03	50
Cobalt (Co)	µg/L	3.1	1.5	0.07	< 0.04	< 0.04	5
Copper (Cu)	µg/L	11	5.5	0.51	0.33	< 0.03	1000
Nickel (Ni)	µg/L	12	5.3	0.33	0.68	0.32	20
Selenium (Se)	µg/L	< 0.05	< 0.05	< 0.05	0.068	< 0.05	10
Zinc (Zn)	µg/L	13	7.8	< 0.3	0.36	2.5	100

Table 10. Content of inorganic ions and trace metals at the five locations visited.

The analysis results may be influenced by the amount of suspended sediments in the samples, which varied considerably between locations as evident from Fig. 23. The samples were left to settle for 1-2 hours before transfer and acidification of 30 mL used for the metals analysis. A significant fraction of the sediment particles were still in suspension at this point in time, though, and could potentially have released additional metals to the water at the time of acidification. If proceeding to a production of drinking water, these suspended particles would presumably be removed prior to distribution and thus only already dissolved metals would influence the quality of the distributed water. By carrying out the trace metals analysis after 1-2 hours of sedimentation, we have ensured that the results can be considered as worst-case at the time of the sampling. This implies that e.g. L-25 could in reality have a significantly lower content of cobalt and nickel than the current results indicate.

For this reason, performing an additional analysis for trace metals on filtered samples should be considered in case locations are revisited. For the locations L-06, L-07 and L-08b we would expect the content of trace metals to be higher later in the melt season, when the

contribution from glacial meltwater relative to snowmelt is significantly higher than at the time of the sampling from which results are presented here. We therefore recommend that these three locations should be revisited at a later time in the melt season, to ensure that they are indeed as low on trace metal content as indicated.



Figure 23. *The difference in the sediment content of the water from the locations are easily discernable. The samples were left for sedimentation for 1-2 hours before transfer and acidification of 30 mL for analysis for metals. A large part of the particles were still in suspension at this point in time and may potentially have released additional metals to the water during acidification.*

6.3 Radioisotopes

Radioactivity from natural mineral sources is unwanted in drinking water and is generally not expected to be an issue. Yet, occurrences of radioactive minerals do exist in parts of Greenland and it was therefore chosen to include analysis of the most common radioactivity parameters, which for the EU and Denmark is 'total indicative dosis' and 'tritium' and for the International Council of Bottled Water Associations is 'total alpha- and beta-activity' (see Table 11). A weak beta-activity hovering around the detection limit was observed for L-04 and L-07, but with values far below the required threshold level. Apart from these, all analyses yielded values below the detection limit of the laboratories and thus easily meeting the quality requirements. Radioactivity in water originates from specific minerals and may for this reason be tied to sediment particles, which at the time of sampling was virtually non-existing at L-06, L-07 and L-08b. These locations should thus be revisited later in the melt season to ensure that the low values extend over the whole melt season.

Parameter	Unit	L-25	L-04	L-06	L-07	L-08b	Criterion*
Total indicative dosis	mSv/yr	< 0.1	< 0.1	< 0.1	< 0.1	< 0.1	0.1
Tritium activity	Bq/l	< 7	< 7	< 7	< 7	< 7	100
Total alpha-activity	Bq/l	0.03	0.04	< 0.02	< 0.03	< 0.02	0.1
Total beta-activity	Bq/l	< 0.15	0.13	< 0.14	0.14	< 0.15	1.0

* Total indicative dosis and tritium as regulated in the EU and Denmark. Total alpha and beta as indicated in the International Council of Bottled Water Associations standards (ICBWA).

Table 11. Radioactivity parameters.

6.4 Bacterial counts

When water is bottled, it should as a minimum fulfil the Danish microbiological criteria described in "Bekendtgørelse om naturligt mineralvand, kildevand og emballeret drikkevand" (BEK nr 38 af 12/01/2016). These analyses should be carried out in an accredited laboratory.

Parameter	Guideline value
<i>Escherichia coli</i> (<i>E. coli</i>)	0/250 ml
Coliform bacteria	0/250 ml
Enterococci (<i>Enterococcus faecalis</i>)	0/250 ml
<i>Clostridium perfringens</i> (herunder sporer)	0/100 ml
<i>Pseudomonas aeruginosa</i>	0/250 ml
Pathogenic microorganisms	Not detected
CFU* at 22°C	100/ml
CFU at 36°C	20/ml

* Colony forming units

Table 12. Microbiological guideline values for bottled water (BEK nr 38 af 12/01/2016).

CFU counts should be performed within 24 hours by the accredited laboratory, which is not possible with the logistical challenges during fieldwork conducted over large distances in Southwest Greenland. We have therefore made a more simple screening at field condition using the Petrifilm method. Results from this method are not as certain as when the samples are analyzed in an accredited laboratory and the detection limits are higher. We have used petrifilm to analyze total CFU (3M petrifilm Aqua 6450/6452 heterotrophic at 22°C), thermotolerant CFU (3M petrifilm Aqua 6450/6452 heterotrophic at 36°C), coliform bacteria (3M petrifilm Aqua 6457/6458 coliform) and bacteria from the group Enterobacteriaceae (3M petrifilm Aqua 6418/6428 Enterobacteriaceae).

According to the guideline, CFU counts should be incubated at constant temperatures (22 ±2°C for 72 h, 36 ±2°C for 24 h), which is a challenge in field conditions without access to 220V electricity. Incubations of the samples are as far as possible made as described in

DS/EN ISO 6222, with the deviation that CFU are determined with petrifilm instead of seeding in agar made from yeast extract. The ISO standard notes that CFU should be incubated at $22 \pm 2^\circ\text{C}$ for 68 h and at $36 \pm 2^\circ\text{C}$ for 44 ± 4 h, so there is a deviation between the ISO-standard and the guideline (Table 12) concerning thermotolerant CFU. Petrifilm for counting coliform bacteria and *Enterobacteriaceae* is likewise incubated for $36 \pm 2^\circ\text{C}$ but only for 21 ± 3 hours, as described in DS/EN ISO 9308-1, whereafter they are moved to a chilled keep and counted within 12 hours.

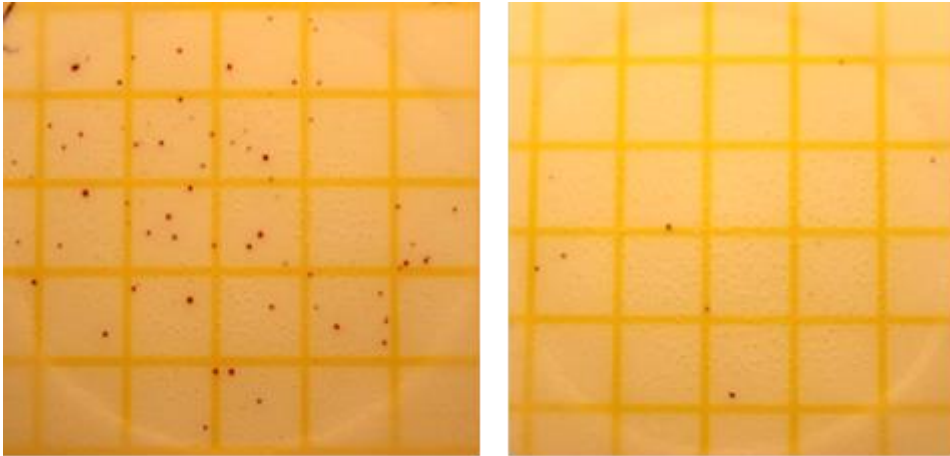


Figure 24. Example of petrifilm results for heterotrophic CFU at 22°C , undiluted (left) and 10x-diluted (right).

The petrifilms were incubated in custom-made, mobile incubators (Fig. 25), since the power source available was 12V lead-acid batteries. The temperature in the 36°C -incubator varied from 34 to 38°C , which seems acceptable and within the prescription of the ISO-standard. The 22°C -incubator had to be constructed without heat-cable, since the heat-cable ordered never arrived before the fieldwork. A 12V light bulb was used instead, however the heat from the bulb was not always sufficient, hence the temperature in the 22°C -incubator was occasionally too low. Most of the time, the temperature was between 18 and 24 , which is not exactly as prescribed in the ISO-standard ($22 \pm 2^\circ\text{C}$), but this is not expected to have influenced the CFU number significantly.



Startzeit/Start time	14-06-2017 00:05:15	Start durch/Start by
Stoppzeit/Stop time	14-06-2017 15:47:15	Stopp-durch/Stop by
Datensätze/Records	472	Dauer/Duration
Temperatur/Temperature	Min 32.4 °C Avg 36.5 °C Max 36.9 °C	
Feuchtigkeit/Humidity	17.3 %rH 32.2 %rH 30.1 %rH	
Taupunkt/Dew point	7.9 °C 11.3 °C 15.6 °C	
Alarm/Alarm	Anzahl/Count	0

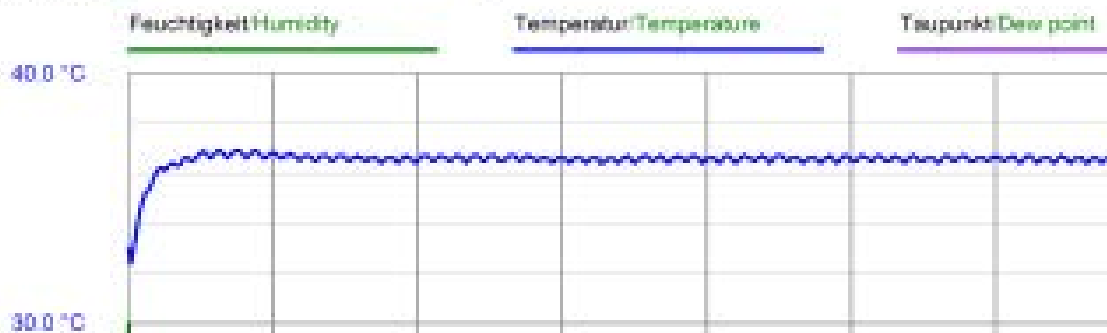


Figure 25. Incubators (polystyrene boxes) (photo in top panel) and example of temperature curve during incubation at 36°C (bottom panel).

Coliform bacteria are a group of bacteria, of which many are intestinal. Since *E. coli* is a subgroup of the coliform bacteria, this means that if no coliform bacteria are present, there are also no *E. coli* in the samples. *Enterobacteriaceae* is a broad group of bacteria, of which many are intestinal. The presence of coliform and/or *Enterobacteriaceae* therefore indicates if there is fecal contamination. The counts for fecal indicator species performed on-site are not exactly as those demanded in the microbiological guideline for bottled water (BEK nr 38 af 12/01/2016), but are judged sufficient for a screening phase.

The results from the bacterial analyses are shown in Table 13. L-04, L-07, L-8b and L-25 had few heterotrophic CFU, below the threshold limit at 22 and 36°C. In these samples, there was also no sign of fecal contamination, but it should be noted that the detection limit was higher than prescribed in the guideline. L-06, on the other hand, exceeded the guideline value for heterotrophic CFU at 22°C. Likewise, in this sample, *Enterobacteriaceae* were detected, indicating fecal contamination. The exceedances can be due to local contamination such as bird droppings or may be due to a more wide-spread contamination. Based on a single sample, we cannot determine which of the possibilities is correct. If this site is assessed to be suitable based on other parameters, it is recommended to monitor the development in heterotrophic CFU and fecal contamination indicators throughout an entire melt season.

For all sites, assessed to be suitable for production, we recommend to follow those microbiological parameters prescribed in the guideline (Table 12) at repeated analyses throughout an entire season. The microbiological parameters should be determined at an accredited laboratory. If a site is chosen for production, we furthermore recommend to make repeated measurements of intestinal parasites (*Cryptosporidium*).

	L-25	L-04	L-06	L-07	L-08b
Heterotrophic, 22°C (CFU/mL)	35±3	67±3	115±5	7±1	15±2
Heterotrophic, 36°C (CFU/mL)	< 0.2	0.6±0.3	0.4±0.3	< 0.2	1.6±0.6
Coliform, 36°C (CFU/5 mL)	0	0	0	0	0
<i>Enterococcaceae</i> , 36°C (CFU/5 mL)	0	0	2	0	0

Table 13. Bacterial counts made with petrifilm during field conditions.

6.5 Cyanotoxins

Cyanobacteria are often the dominating, photosynthesizing bacteria in aquatic freshwater ecosystems in the Arctic (Callieri et al., 2012; Vincent et al., 2012). Cyanobacteria can under certain circumstances produce large amounts of toxins of which microcystins (also known as cyanoginosins) is the most well-studied group (WHO, 2011). In contrast to many other cyanotoxins, microcystins are often cell-bound substances, which means that they to some extent may be removed during sedimentation processes (WHO, 2011). A research paper from 2016 reported the presence of microcystins in 18 out of 18 lakes in Western Greenland (Trout-Haney et al., 2016). The levels varied from 0.005 to 0.4 µg/L. Based on those findings, the water samples were analyzed for microcystins at a commercial lab. The cyanotoxins AnatoxinA and nodularin were included as well. No cyanotoxins were detected in any of the samples (Table 14). This result does not rule out completely the presence of cyanotoxins, since the detection limit at the commercial lab was 0.5-2.0 µg/L, which is higher than all findings in 2016. The analytical method used in the 18 lakes in 2016 was an immunochemical method (ELISA), with a very low detection limit. However, it does not discriminate between different microcystins and also provides a signal for nodularin, which has

a similar chemical structure. Since earlier data were based on a different analytical principle, the results from 2016 are not directly comparable with the results in Table 14.

Microcystin LR is the most widespread cyanotoxin and the only cyanotoxin, where sufficient data exist to make a threshold limit (WHO, 2011). The provisional guideline value for microcystin LR (free + cell-bound) in drinking water is 1 µg/L (WHO, 2011). This value is not exceeded at any of the selected locations, but it needs to be pointed out that other microcystins may be present without detectable levels of microcystin LR. A substantial seasonal variation must be expected and we therefore recommend to monitor cyanotoxins throughout a season at a potential production location.

Parameter	Unit	L-04	L-06	L-07	L-08b	L-25
Anatoxin A Fumarate	µg/L	< 0.5	< 0.5	< 0.5	< 0.5	< 0.5
Microcystin LW	µg/L	< 2	< 2	< 2	< 2	< 2
Microcystin LR	µg/L	< 0.5	< 0.5	< 0.5	< 0.5	< 0.5
Microcystin RR	µg/L	< 0.5	< 0.5	< 0.5	< 0.5	< 0.5
Microcystin YR	µg/L	< 0.5	< 0.5	< 0.5	< 0.5	< 0.5
Nodularin	µg/L	< 0.5	< 0.5	< 0.5	< 0.5	< 0.5

Table 14. *Cyanotoxin analyses.*

6.6 Sediment content

When flying over Greenland, it is impossible not to notice how the lakes vary in colour, from clear and dark to blueish, "milky", grey and brown. The difference in colour is due to the variation in the content of sediment (rock in particle form), which is found in different concentrations (mg/L) in the water. Rivers may also differ quite substantially; in some valleys, rivers wind through green areas within a single riverbed whereas in other valleys, rivers form vast networks of braided (flettede) channels taking up the entire vegetation-free valley floor. When investigating the origin of the braided river systems, they most often derive from local glaciers or the inland ice. The erosion of the glacier ice of the basal material produces the sediment as the glacier moves over the terrain. This form of erosion is one of the most powerful on the Earth. Water originating from melting local glaciers or the Greenland Ice Sheet will thus always contain a certain amount of sediment.

The largest concentrations of sediment are observed where the meltwater leaves the glacier. The concentration of sediment decreases downstream if the sediment-laden water passes lakes where part of the sediment will settle on its way towards the sea. Often, the sediment-rich water reaches all the way to the ocean, where sediment plumes colour the water in front of the river mouths. The sediment content has an influence on the quality and use of the water for drinking or industrial purposes.

Collected water samples for suspended sediments are from sites representative of the remaining water sampling. The water samples are taken at locations where all sediment-laden water passes, with an emphasis on obtaining well-mixed water.

Sediment content is expressed by a concentration, i.e. the content of rock material in mg per litre of water. Additional information on the size distribution of the particles is also obtained. Results are shown in Table 15. Examples of particle size distribution of the samples from the two stations with the largest sediment concentration are in Fig. 26.

Parameter	Unit	L-25	L-04	L-06	L-07	L-08b
Suspended sediment	mg/L	165	95	1.2	0.7	0.5
Temperature	°C	3.7-4.4	4.6	3.8-4.2	2.6	1.5
Conductivity	µS/cm	16	15	13	23	15
Time of day (UTC-2)	WGST*	13:15	11:10	09:50	13:00	09:40
Estimated discharge**	m ³ /s	50	40	5-10	5-10	5-10

*Western Greenland Summer Time (Daylight Saving Time) is UTC – 2 hours.

**Judged by field participants as a simple visual estimate.

Table 15. *The sediment content and related parameters of water samples.*

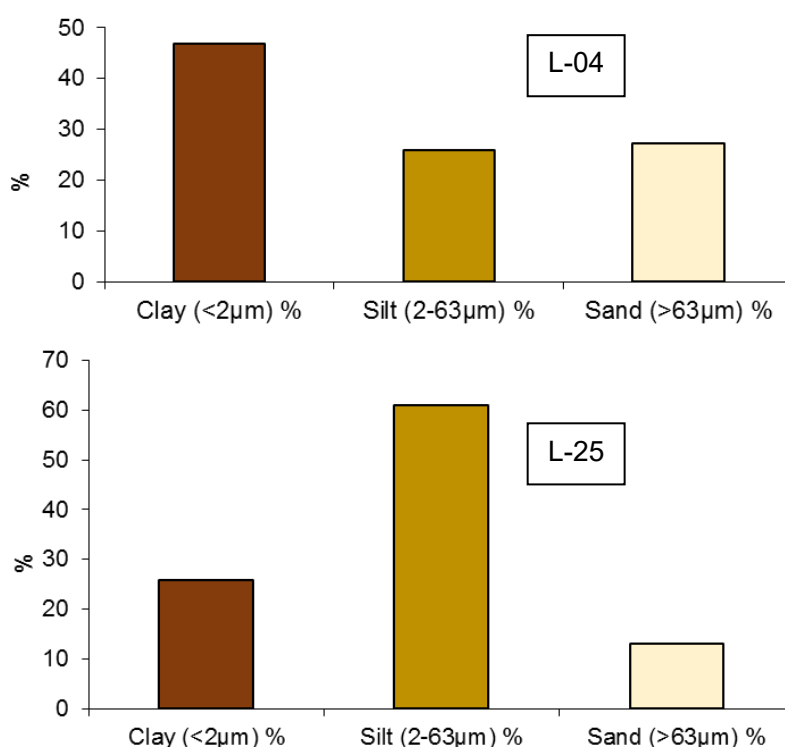


Figure 26. *The size distribution of the suspended sediment in water samples from L-04 (top panel) and L-25 (bottom panel) when divided into three well-defined types of particles.*

According to the Danish Environmental Agency (BEK nr. 1147), the requirement for drinking water at the point of use is 1 FNU (Formazin Nephelometric Unit), corresponding to approx. 2 mg/L of suspended sediment, but may be 0-3 mg/L (see DS/EN ISO 7027).

Two concentrations observed in the collected water samples clearly exceed the 1 FNU limit, equal to 0-3 mg/L. Thus, sediment must be removed in order to fulfil the required standard. The other three locations are at or below the limit.

Here we have employed suspended sediment concentration (mg/L) instead of FNU in order to be able to calculate the weight of transported suspended sediment by multiplying the concentration with discharge (m^3/s). The samples L-25 and L-04 clearly show glacial origin while samples from to other locations have quite low concentrations due to settling before reaching the sampling location.

The grain size distributions in Fig. 26, show that the largest proportion of the transported sediment consists of grain sizes finer than sand. Large particles settle more easily, while finer grained sediment settles slowly and are thus more likely to be transported all the way to the sea before they settle.

7. Conclusion

This report contains information on five selected locations that may be utilized for industrial collection of drinking water. A prerequisite in the investigation has been that the water should be at least partly derived from meltwater originating either from the Greenland Ice Sheet or from local glaciers and ice caps. The five locations presented here were all visited in the field in June 2017, after an initial screening of possible sites. Since glacial meltwater running in meltwater rivers towards the fjords has been in contact with the base of the glacier or the river bed, it generally contains suspended sediment that must be filtered out before the water can be used for drinking purposes. This report is not aimed at addressing any technical or engineering questions posed by the locations or water treatment, but only concerns the natural environment and the quality of the water as it was sampled.

Visiting the locations in June was a compromise, as the meltwater rivers will contain both water from snowmelt and melting ice, with the division depending on geographical location and local conditions. This timing captures any issues that may arise from water quality parameters derived from snowmelt over the ice-free part of the catchment. An example of this is animal droppings, frozen in the snow over the winter, but potentially being released as the snow melts in the early summer. Ideally, a complementary visit should be conducted later in the season to better capture other water quality parameters, which are more relevant later in the season. If a location is chosen for further exploration, we recommend regular sampling over the melt season.

The five locations presented here differ substantially in the type of setting and in their water quality parameters. Whether a specific location is more suitable than another entirely depends on the intended exploration model, both with respect to technical solutions and in terms of chosen business model. Some locations, like L-04 and L-25, discharge huge amounts of meltwater derived from the Greenland Ice Sheet, but also has the highest sediment load and more challenging access in terms of water depth, access to waterfall and distance to populated areas. Other locations, like L-06, L-07 and L-08b are closer to populated areas, which can be both an advantage and a disadvantage, and have easier access in terms of water depth. However, these locations also discharge less water and the meltwater is derived from local glaciers rather than the Greenland Ice Sheet itself.

8. References

Aschwanden, A., E. Bueller, C. Khroulev and H. Blatter (2012), An enthalpy formulation for glaciers and ice sheets, *Journal of Glaciology* 58(208).

Bekendtgørelse om naturligt mineralvand, kildevand og emballeret drikkevand" (BEK nr 38 af 12/01/2016).

bkg_nr_07_2008_bilag3a_dk pdf (analyseprogram kemiske parametre for Grønlandsk drikkevand). Fra: Hjemmestyrets bekendtgørelse nr. 7 af 17. marts 2008 om vandkvalitet og tilsyn med vandforsyningsanlæg.

bkg_nr_07_2008_bilag1b_dk pdf (generelle og uorganiske parametre i Grønlandsk drikkevand). Fra: Hjemmestyrets bekendtgørelse nr. 7 af 17. marts 2008 om vandkvalitet og tilsyn med vandforsyningsanlæg.

Bueller, E, and J. Brown (2009), Shallow shelf approximation as a "sliding law" in a thermodynamically-coupled ice sheet model, *Journal of Geophysical Research* 114.

Callieri, C., Cronberg, G. and Stockner, J. Chapter 8: Freshwater picocyanobacteria: Single cells, Microcolonies and colonial forms. In *Ecology of Cyanobacteria II: Their Diversity in Space and Time*; Whitton, B.A., Ed.; Springer: Dordrecht, The Netherlands, 2012; pp. 229–261.

Christensen, O., Drews, M., Christensen, J., Dethloff, K., Ketelsen, K., Hebestadt, I., et al. (2006). The HIRHAM regional climate model, version 5. Available at: <http://www.dmi.dk/fileadmin/Rapporter/TR/tr06-17.pdf>.

Dee, D. P., Uppala, S. M., Simmons, A. J., Berrisford, P., Poli, P., Kobayashi, S., et al. (2011). The ERA-Interim reanalysis: configuration and performance of the data assimilation system. *Q.J.R. Meteorol. Soc.* 137, 553–597. doi:10.1002/qj.828.

DS/EN ISO 6222:2000. Vandundersøgelse. Bestemmelse af antal mikroorganismer i gærestraktagar ved 22°C og 36°C. Dybdeudsæd.

DS/EN ISO 9308-1:2014 Water quality -- Enumeration of *Escherichia coli* and coliform bacteria.

Eerola, K. (2006). About the performance of HIRLAM version 7.0. *HIRLAM Newsletter* 51, 93–102.

Ettema, J., M.R. van den Broeke, E. van Meigaard, W.J. van de Berg, J.L. Bamber, J.E. Box and R.C. Bales (2009), Higher surface mass balance of the Greenland ice sheet revealed by high-resolution climate modeling, *Geophys. Res. Lett.*, 36, L12501, doi:10.1029/2009GL038110.

EPA. 2016: Ground Water and Drinking Water. Table of Regulated Drinking Water. Contaminants. 15pp.

EU. 2013: Rådets Direktiv 2013/51/EURATOM af 22. Oktober 2013 om krav til beskyttelse af befolkningens sundhed med hensyn til radioaktive stoffer i drikkevand. 10pp.

International Council of Bottled Water Associations standards. ICBWA Model Code. September 27. 2004.

Howat, I.M., A. Negrete, and B.E. Smith, 2014, The Greenland Ice Mapping Project (GIMP) land classification and surface elevation datasets, *The Cryosphere*, 8, 1509-1518, doi:10.5194/tc-8-1509-2014.

Langen PL, Fausto RS, Vandecrux B, Mottram RH and Box JE (2017) Liquid water flow and retention on the Greenland ice sheet in the regional climate model HIRHAM5: Local and large-scale impacts. *Frontiers in Earth Science*, 4 (doi:10.3389/feart.2016.00110)

Mayer, C.J., C.E. Bøggild, O.B. Olesen and S Podlech (2003) Ice studies in relation to ice/water export, data collection, modelling and evaluation approach, Danmarks og Grønlands Geologiske Undersøgelse Rapport 2003/6, 33pp

Morlighem, M., E. Rignot, J. Mouginot, H. Seroussi and E. Larour. 2015. IceBridge BedMachine Greenland, Version 2. Boulder, Colorado USA: NASA DAAC at the National Snow and Ice Data Center. <http://dx.doi.org/10.5067/AD7B0HQNSJ29>.

Morlighem, M., E. Rignot, J. Mouginot, H. Seroussi and E. Larour. 2014. Deeply incised submarine glacial valleys beneath the Greenland Ice Sheet, *Nature Geoscience*, 7:418-422. doi:10.1038/ngeo2167.

Nöel, B., W.J. van de Berg, H. Machguth, S. Lhermitte, I. Howat, X. Fettweis and M.R. van den Broeke (2016): A daily, 1-km resolution dataset of downscaled Greenland ice sheet surface mass balance (1958--2015), *The Cryosphere*, 10, 2361-2377.

Rambøll 2006. Grønlandsk is og vand. Opgave 1: Bilagsrapport B. Kortlægning af vandressourcer.

Reeh, N., H. Oerter and H.H. Thomsen (2002) Comparison between Greenland ice-margin and ice-core oxygen-18 records. *Annals of Glaciology*.

Roeckner, E., Bäuml, G., Bonaventura, L., Brokopf, R., Esch, M., Giorgetta, M., et al. (2003). The atmospheric general circulation model ECHAM5. Part I: Model description. Available at: http://www.mpimet.mpg.de/fileadmin/publikationen/Reports/max_scirep_349.pdf.

Trout-Haney, J.V., Z.T. Wood and K.L. Cottingham. 2011. Presence of the Cyanotoxin Microcystin in Arctic Lakes of Southwestern Greenland. *Toxins* 8: 256; doi:10.3390/toxins8090256.

Vincent, W.R. and Quesada, A. Chapter 13: Cyanobacteria in high latitude lakes, Rivers, and seas. In *Ecology of Cyanobacteria II: Their Diversity in Space and Time*; Whitton. B.A.. Ed.; Springer: Dordrecht. The Netherlands. 2012; pp. 229–261.

WHO. 2011. *Guidelines for Drinking-water Quality*. Fourth edition.

WHO. 1999. *Toxic Cyanobacteria in Water: A guide to their public health consequences, monitoring and management*. Edited by Ingrid Chorus and Jamie Bartram. http://www.who.int/water_sanitation_health/resourcesquality/toxcyanobacteria.pdf.

Winkelmann, R., Martin, M. A., Haseloff, M., Albrecht, T., Bueler, E., Khroulev, C. and Levermann, A. (2011), The Potsdam Parallel Ice Sheet Model (PISM-PIK) Part 1: Model description, *The Cryosphere*, 5 p.715-726.